

Comparative Study of Date seed and Olive Pomace Derived Graphene-like Carbon Synthesis for Potential Application in High Performance Supercapacitors



By
Saima Zameer

School of Chemical and Materials Engineering
National University of Sciences and Technology

2023

Comparative Study of Date Seed and Olive Pomace Derived Graphene-Like Carbon Synthesis for Potential Application in High Performance Supercapacitors



Name: Saima Zameer

Reg: 00000363954

This thesis is submitted as a partial fulfillment of the requirements for the degree of

MS in Chemical Engineering

Supervisor Name: Dr. Waheed Miran

School of Chemical and Materials Engineering (SCME)

National University of Science and Technology (NUST)

H-12, Islamabad, Pakistan

August, 2023



THESIS ACCEPTANCE CERTIFICATE

Certified that final copy of MS thesis written by Ms **Saima Zameer** (Registration No 00000363954), of School of Chemical & Materials Engineering (SCME) has been vetted by undersigned, found complete in all respects as per NUST Statues/Regulations, is free of plagiarism, errors, and mistakes and is accepted as partial fulfillment for award of MS degree. It is further certified that necessary amendments as pointed out by GEC members of the scholar have also been incorporated in the said thesis.

Signature: Waheed Miran

Name of Supervisor: Dr Waheed Miran

Date: 12/10/2023

Signature (HOD): [Signature]

Date: 12/10/23

Signature (Dean/Principal): AA

Date: 12-10-2023

National University of Sciences & Technology (NUST)

MASTER'S THESIS WORK

Formulation of Guidance and Examination Committee (GEC)

Name: Saima Zameer NUST Reg No: 00000363954
 Department: Department of Chemical Engineering Specialization: Master of Science in Chemical Engineering
 Credit Hour Completed: 24.0 CGPA: 3.63
 Course Work Completed

S.No	Code	Title	Core/Elective:	CH:	Grade:
1.	CHE-843	Separation Processes In Che	Compulsory	3.0	B
2.	CHE-847	Chemical Kinetics & Reactor Design	Compulsory	3.0	B+
3.	RM-898	Research Methodology	Additional	2.0	Q
4.	CHE-848	Gasification Processes	Elective	3.0	A
5.	CHE-823	Advance Analytical Techniques	Elective	3.0	B+
6.	EME-921	Momentum Heat & Mass Transfer In CHE	Compulsory	3.0	A
7.	EME-981	Advance Fuel Technology	Elective	3.0	A
8.	CHE-815	Nano Catalysis	Elective	3.0	B+
9.	ESE-800	Clean Coal Technologies	Elective	3.0	B+

Student's Signature *AZ*

Date: 09 - Feb - 2023

Thesis Committee

Name: Waheed Miran (Supervisor)
 Department: Department of Chemical Engineering
 Name: Tayyaba Noor (Cosupervisor)
 Department: Department of Chemical Engineering
 Name: Dr. Ameen Shahid (Internal)
 Department: Department of Chemical Engineering
 Name: Usman Liaqat (Internal)
 Department: Department of Materials Engineering

Signature *Waheed*

Signature *Tayyaba*

Signature *Dr. Ameen*

Signature *Usman*

Signature of Head of Department: *E.B.*

Date: 09 - Feb - 2023

APPROVAL

Signature of Dean/Principal: *AJ*

Date: 09 - Feb - 2023



National University of Sciences & Technology (NUST)

FORM TH-4

MASTER'S THESIS WORK

We hereby recommend that the dissertation prepared under our supervision by

Regn No & Name: 00000363954 Saima Zameer

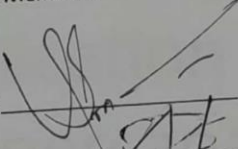
Title: Comparative study of date seed and olive pomace derived graphene-like carbon synthesis for potential application in high performance supercapacitors.

Presented on: 10 Oct 2023 at: 1400 hrs in SCME Seminar Hall

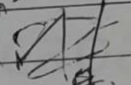
Be accepted in partial fulfillment of the requirements for the award of Master of Science degree in Chemical Engineering.

Guidance & Examination Committee Members

Name: Dr Usman Liaqat

Signature: 

Name: Dr Ameen Shahid

Signature: 


Name: Dr Tayyaba Noor (Co-Supervisor)

Signature: Tayyaba

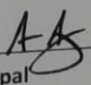
Supervisor's Name: Dr Waheed Miran

Signature: Waheed

Dated: 11/10/2023


Head of Department

Date 11/10/23


Dean/Principal

Date 11.10.2023

School of Chemical & Materials Engineering (SCME)

Dedication

This research is dedicated to my parents, respected teachers, to my family and friends.

Acknowledgment

All praises to Almighty Allah, without His will nothing can happen, who favored us with the capacity to think and made us anxious to investigate this entire universe. Incalculable greetings upon the Holy Prophet Hazrat Muhammad (PBUH), the reason for the creation of the universe and wellspring of information and blessing for whole humankind. From the core of my heart, I am thankful to my research supervisor, Dr. Waheed Miran for his unwavering technical and moral support and enlightening me with a research vision and pushing me for excellence. It is his consistent and encouragement that empowered me to achieve this milestone. I extend my sincere gratitude towards my guidance and committee members: Dr. Tayyaba Noor, Dr Ameen Shahid and Dr. Usman Liaqat for guiding and supporting me in my research course. It would not have been possible without them. Also, I am thankful of my Seniors who shared their knowledge regarding experimental techniques, and they motivated me in this entire research work. I am highly obligated to my Parents and siblings for their never-ending love. Thanks for believing in me, wanting the best for me, and inspiring me to follow my passion. Without them, this journey would not have been accomplished.

(Saima Zameer)

Abstract

In the pursuit of eco-friendly and sustainable energy storage devices, supercapacitors have gain a lot of attention due to their long cycle life, fast charge/discharge rate and high power density. The performance of the supercapacitors is mainly based on the properties of the electrode material, such as carbon based electrodes, mainly graphene-based electrode material serves as the promising candidates. Cleaner ways for synthesis of graphene-like carbon are highly expected. Renewable resources such as date seed and olive pomace serves for this purpose. The research is based on a comparative study of two unconventional biomass resources, date seed and olive pomace, for the graphene-like carbon synthesis and evaluate their application as electrode material for supercapacitors. Graphene-like carbon were synthesized via hydrothermal carbonization followed by acid washing. Electrochemical testing was performed to evaluate olive pomace and date seed derived graphene-like carbon performance of the synthesized electrode material. The electrochemical testing results showed that the specific capacitance of 502 F/f & 460 F/g in three cell electrode testing, respectively. Moreover, the olive pomace derived graphene-like carbon gave the better results and was further evaluated in two cell electrode testing it gave the specific capacitance of 518F/g. The electrode material was highly stable and retained the capacitance retention of 96% even after 1000 cycles. Thus, olive pomace derived graphene-like carbon served as the promising material as electrode material for the application in supercapacitors.

Table of Contents

Dedication	i
Chapter 1:	1
Renewable Energy Resources	2
Energy storage device	2
1.1.1 Batteries	3
1.1.2 Fuel cells	3
1.1.3 Capacitors	4
1.1.4 Supercapacitors	5
Lignocellulosic Biomass resources and types	7
1.1.5 Cellulose	9
1.1.6 Hemicellulose	9
1.1.7 Lignin	9
Research Problem	9
Research Objectives	10
Chapter 2:	11
Literature Review	11
Graphene-like carbon Synthesis	11
2.1.1 Carbonization	11
2.1.2 Hydrothermal Carbonization	13
Chapter 3:	16
Methodology	16
Synthesis of graphene-like carbon from olive pomace and date seed	16
3.1.1 Chemicals	16
3.1.2 Procedure	16
Materials Characterization	17
3.1.3 Ultimate and proximate analysis	17
3.1.4 XRD	17
3.1.5 SEM	17

3.1.6	EDX-----	17
3.1.7	Raman spectroscopy -----	17
3.1.8	FTIR -----	17
	Electrodes Preparation -----	17
	Electrochemical Testing -----	18
	Chapter 4:-----	19
	Results & Discussion-----	19
	Physicochemical Characterization -----	19
4.1.1	XRD -----	21
4.1.2	Raman spectroscopy -----	22
4.1.3	FTIR -----	23
4.1.4	SEM-----	24
4.1.5	EDX-----	25
	Electrochemical Testing Results -----	26
4.1.6	Three cell electrode testing -----	26
4.1.7	Two cell electrode testing -----	32
	Conclusion -----	38
	Recommendations -----	39
	References-----	40

Table of Figures

Figure 1-1 Rangone plot for energy storage devices	2
Figure 1-2 Schematic of working batteries	3
Figure 1-3 Working of a fuel cell	4
Figure 1-4 Types of supercapacitors	5
Figure 1-5 Schematic of EDLC supercapacitors	6
Figure 1-6 Schematic of pseudo capacitors.....	7
Figure 2-1 Synthesis representation of PS-FLG and its successive incorporation into a solid-state supercapacitor	12
Figure 2-2 illustrates the process of producing graphene nanosheets using brown-rice husks as the source material.	13
Figure 2-3 The synthesis mechanisms and methods for enhancing the electrochemical properties of graphene-like active carbon are illustrated in the figure, with arrows highlighting the ion transport pathways in C-H ₂ O, C-H ₂ O ₂ , C-HAc, and C-H ₂ O ₂ /HAc.	14
Figure 4-1 Schematic diagram for synthesis of graphene-like carbon.....	20
Figure 4-2 (a) Proximate analysis of OP and DS, (b) Ultimate analysis of DS, DS-800, OP, OP-800.....	20
Figure 4-3 XRD pattern of OP 800 and DS 800.....	21
Figure 4-4 Raman spectra of OP 800 and DS 800.....	22
Figure 4-5 FTIR analysis of OP 800 & DS 800	23
Figure 4-6 (a & c) SEM images of precursor OP and DS. (b) SEM image for synthesized graphene-like carbon from OP at 800°C (c) SEM image for synthesized graphene-like carbon from DS at 800°C.....	24
Figure 4-7 EXD analysis of samples (a & c) EXD analysis of raw DS and OP (b) exhibits the EDX composition of DS 800 (d) EXD of OP 800.....	25
Figure 4-8 (a) CV curves of OP 800 at different scan rates (b) CV curves of DS 800 at different scan rates	26
Figure 4-9 Comparison of CV curves of OP 800 and DS 800 at the scan rate of 100 mV/s	27
Figure 4-10 GCD curves of OP 800 at different current densities (b) GCD curves of DS 800 at different current densities	28
Figure 4-11 GCD curves of OP 800 and DS 800 at the current density of 0.5 A/g	29

Figure 4-12 (a) Specific capacitance of OP 800 & DS 800 at different current densities (b) Nquist plot for as-prepared materials	30
Figure 4-13 CV curves of OP 800 at different scan rates	32
Figure 4-14 GCD curves of OP 800 at different scan rates.....	33
Figure 4-15 Specific capacitance of OP 800 at different current densities	34
Figure 4-16 Ragone plot for as-prepared symmetric supercapacitor.....	34
Figure 4-17 Nquist plot for OP 800	35
Figure 4-18 Capacitance retention of OP 800 in IM electrolyte after 1000 cycles at 5 A/g.....	36

List of Tables

Table 1-1 Advantages of lignocellulosic resources over traditional resources	8
Table 2-1 Various lignocellulosic biomass feedstocks synthesize Graphene like carbon by carbonization method and their electrochemical performance for supercapacitors.....	15
Table 4-1 ERS and RCT vales of as prepared samples of OP 800 & DS 800	31
Table 4-2 Electrochemical performance of activated carbon synthesized from different biomass feedstocks via carbonization and hydrothermal carbonization.....	37

Chapter 1:

Introduction

A significant energy crisis currently exists throughout the world. Progress towards effective and sustainable green energy sources is essential [1]. The world's energy resources are gradually depleting as a result of an expanding human population and advancements in energy use. The amount of dependency on petroleum-based products, such as coal gas and regular oil, is rising at an alarming rate. Petroleum derivatives are disproportionately depleting as a result. Furthermore, the consumption of these materials results in the production of gases like CO₂, SO_x, and NO_x that endanger human life and pollute the environment. These gases are produced as a result of global warming and the greenhouse effect. The health of people is being negatively impacted by this pollution [2]. Among the substances that seriously harm human health and pollute the environment are heavy metals and organic dyes. Water contamination has spread throughout the world because automatic cleaning systems have a limited capacity and untreated industrial waste is dumped into these water bodies as well. Maintaining a cleaner, greener environment is now essential.

With the depletion of nonrenewable energy sources like fossil fuels and petroleum, the renewable energy resources have been concentrated on resolving the energy issue. Numerous materials that produce renewable energy while also being cost-effective are now being tested [3]. In order to reduce environmental contamination, it is vital that we develop ecologically friendly and green technologies. Solar cells, fuel cells, supercapacitors, and other environmentally friendly materials and devices have been produced in recent years with the potential to produce renewable energy and store it for a long period of time [4-7]. Due to rising energy consumption and a reliance on portable energy sources, higher energy and power densities are needed [8, 9]. Fig 1-1 shows the current state of devices which are being used as energy storage.

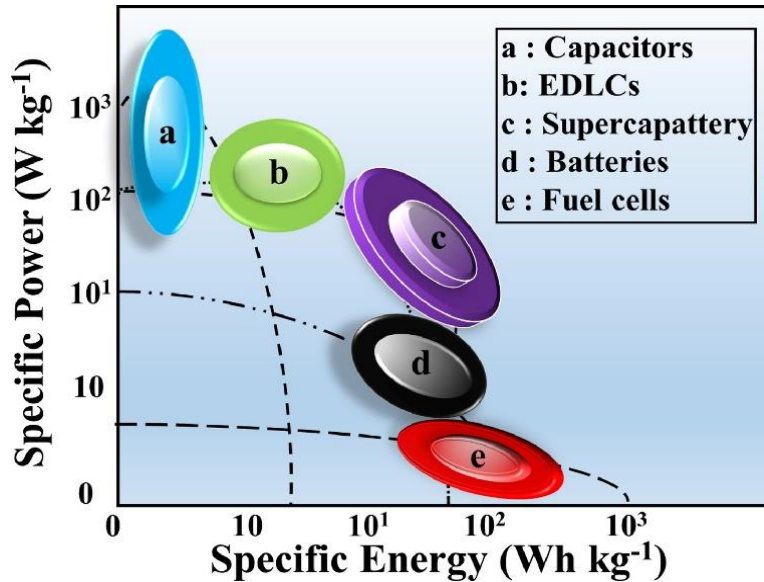


Figure 1-1 Ragone plot for energy storage devices [10]

Renewable Energy Resources

Our reliance on nonrenewable energy sources is reduced by renewable energy sources. These resources are never exhausted and can be utilized once more for our convenience. There are numerous forms of energy which are renewable e.g., biomass, geothermal energy etc.

Energy storage device

Future energy demand and more renewable resources developed there is a strong need for devices which can store energy. Energy storage systems are becoming more necessary as the available resources of biomass energy arises [11].

Energy storage systems are divided into five major categories

- Mechanical system
- Chemical system
- Electrochemical system
- Electrical system
- Thermal system

The most common energy storage devices that come in electrochemical and electrical systems are

- Batteries
- Supercapacitors

1.1.1 Batteries

With the fast development in renewable energy conversion devices, there is a lot of need of electrochemical energy storage devices. Various types of batteries are being used for energy storage applications. The two main categories are as follows.

- (i) Primary batteries
- (ii) Secondary batteries

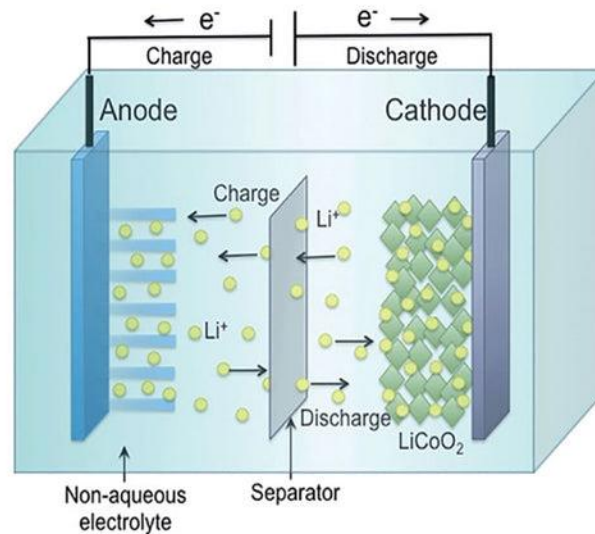


Figure 1-2 Schematic of working batteries [12]

1.1.2 Fuel cells

Fuel cells typically known as energy conversion devices, converts the chemical energy of a fuel and oxidizing agent (typically oxygen) into electricity through multiple redox reactions. These can be further divided into categories based on electrolyte. The ions that are generated during a redox reaction, an electrolyte transfers it from one electrode to the other, making it an essential component of the fuel cells. The electrolytes that are used in a fuel cell are acids, salt carbonates and potassium hydroxide. Some commonly used fuel cells are:

- (i) Polymer exchange fuel cell
- (ii) Solid oxide fuel cell

- (iii) Alkaline fuel cell
- (iv) Carbonate fuel cell
- (v) Phosphoric acid fuel cell

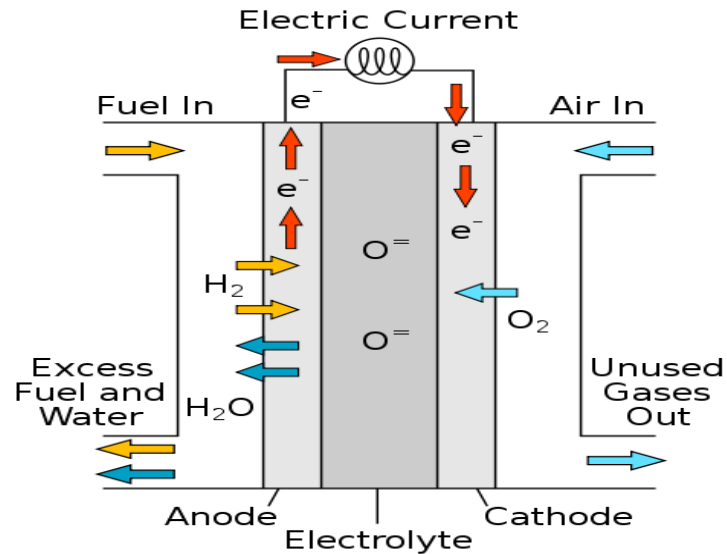


Figure 1-3 Working of a fuel cell [13]

1.1.3 Capacitors

The capacitor is an electrical energy storage device that stores electrical energy in the form of an electric field produced on its electrodes. It is made up of two parallel plates, often known as electrodes, and a dielectric material between the electrodes. Capacitance is defined as a capacitor's ability to store electrical charge, which is computed using the formula

$$Q = CV$$

The geometries of the electrodes used in the capacitor and the type of dielectric used in the capacitor are used to classify the capacitors into distinct types. The most common type of capacitor is the parallel plate capacitor. Two parallel plates of equal area are arranged parallel to each other in this type. The amount of charge that can be stored is determined by the size of the plates and the dielectric substance employed between them. The formula for calculating its capacitance is

$$C = A / d$$

1.1.4 Supercapacitors

An electrochemical capacitor or an electrolytic capacitor are other names for this type of capacitor. In comparison to fuel cells and batteries, it is the most cost-effective device for storing energy with a long cycle life and stability. In comparison to electrochemical batteries and fuel cells, it produces a high amount of power while posing less environmental risks. It consists of two electrodes (anode and cathode), an electrode separator, and an electrolyte. The graphic depicts a schematic of a supercapacitor's operation. A supercapacitor's working principle is quite similar to that of a traditional dielectric capacitor. As an external potential difference V is introduced to the electrode, a charge begins to accumulate. Based on the energy storage technique, it is further divided into three types.

- i. EDLC
- ii. Pseudo capacitors
- iii. Hybrid capacitors

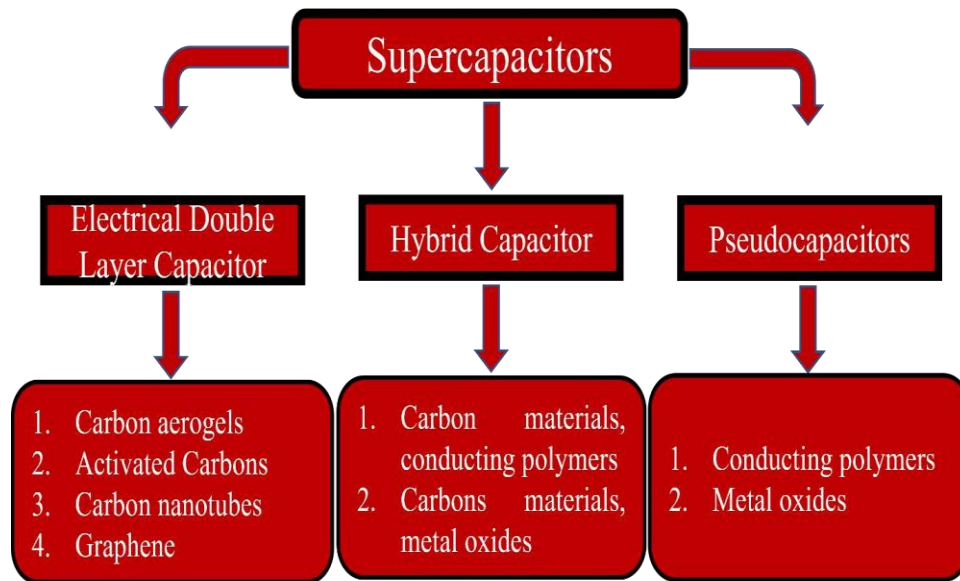


Figure 1-4 Types of supercapacitors

1.1.4.1 Electrochemical double layer capacitors (EDLC)

The mechanism of charge buildup on the electrode-electrolyte interface is used to store electrical energy in the EDLC. The large surface area ensures optimum contact between the active material and the electrolyte at the interface, allowing charge to be sustained. The electrons flow from the cathode to the anode due to the external applied potential difference, and the cation moves from

the anode to the cathode during the charging process of an electron double layer capacitor. During the discharge process, electrons flow backwards. There is no chemical redox process involved in this sort of supercapacitor.

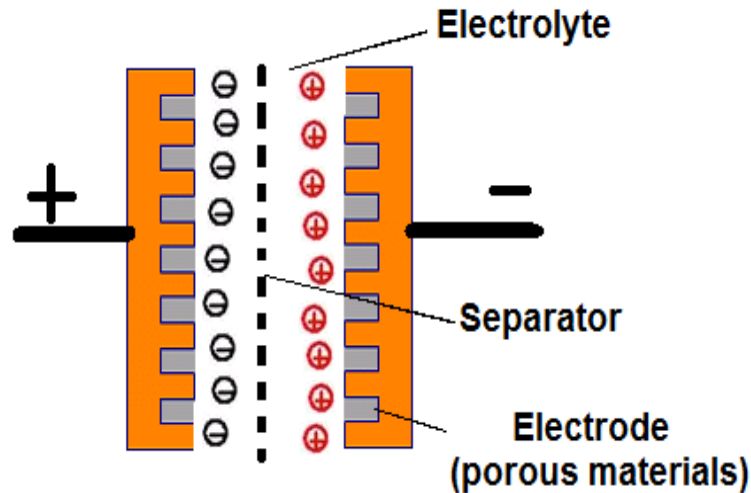


Figure 1-5 Schematic of EDLC supercapacitors [14]

1.1.4.2 Pseudo capacitors

Due to its functioning principle, this type of supercapacitor differs from the EDLC. At the contact of the active substance, chemical redox processes are engaged. The ability to produce a redox reaction under the influence of an externally supplied charge is required for material selectivity for supercapacitor electrodes. Organic compounds (polyaniline and polypyrrene), metal oxides (NiO, Co_3O_4 , CuO, and NiCo_2O_4 etc.), and metal sulfides (MoS_2) are among the materials used in pseudo capacitors. The merits of these are energy density, low cost and capacitance.

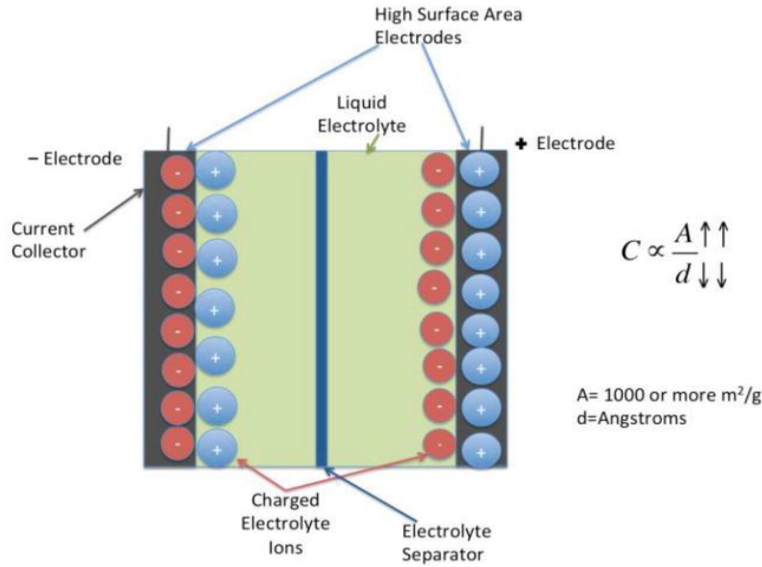


Figure 1-6 Schematic of pseudo capacitors [15]

1.1.4.3 Hybrid supercapacitors

Both pseudo capacitors and EDLCs are used in the design of these supercapacitors. It has two electrodes separated by a semipermeable layer that acts as a separator, preventing electrical contact between them. The electrodes and separator are impregnated with an electrolyte solution that permits ions to pass between them while preventing electrons from discharging the cell.

1.1.4.4 Asymmetric energy storage devices

To attain high energy and power density, asymmetric energy storage devices use both fundamental principles of electron double layer capacitors and batteries. Two different types of electrode materials are used in the asymmetric form of supercapacitors. The first electrode is made up of material that exhibits faradic reaction that provides much high energy density as an anode, while the second electrode is made up of capacitor type material, providing a high-power density.

Lignocellulosic Biomass resources and types

Biomass refers to any substance obtained from agricultural and industrial waste. Typically, cellulose, hemicellulose and lignin are the main constituents of the plant-based biomass materials. Mainly the non-covalent and covalent forces bind together these components. The

main focus of this article is to explore the current research in the field of biomass waste material utilization for the energy storage applications i.e., supercapacitors. The structural and chemical characteristics of lignocellulosic biomass vary depending on the plant species from which it was derived. [Table 1-1](#) lists some of the advantages of lignocellulosic biomass over the traditional sources to generate energy. Lignocellulosic biomasses show a great performance in the electrochemical storage devices and in some other advanced applications like soil and environmental remediation's. The intricate structure of carbon electrodes increases the capacitance of both electrode (negative and positive electrodes), which results in high energy density of the supercapacitors [16]. While some research has focused on replacing redox-active materials over carbon based electrodes to achieve increased capacitance [17-19], this approach may not address the issues of short life cycle and less energy density.

Table 1-1 Advantages of lignocellulosic resources over traditional resources

Sr. No.	Lignocellulosic biomass	Traditional energy sources
1	Renewable nature and abundant availability	Non-renewable in nature and limited supply
2	Reduced pollution	Source for hazardous wastes
3	Lower cost	Expensive
4	Multiple sources	Location-specific
5	Carbon neutral economy	Greenhouse emissions
6	Biodegradable	Non-biodegradable

1.1.5 Cellulose

Cellulose is a widely present organic polymer found in plant cell walls, and it comprises D-glucose units arranged in a six-carbon ring (pyranose) structure. The interaction between the pyranose rings is established by three hydroxyl groups in each ring, which leads to the formation of two types of hydrogen bonds. These bonds are responsible for the remarkable crystalline structure, chemical stability, and mechanical strength of cellulose. Cellulose is also known as anhydrous glucopyranose polysaccharide since the acetal linkages between pyranose rings result in the loss of a water molecule of water [20].

1.1.6 Hemicellulose

Hemicellulose, the polymer that envelops cellulose fibers and links cellulose and lignin, is composed of various monomers such as glucose, galactose, mannose, xylose, arabinose, and glucuronic acid [21]. The presence of 3-methoxy-galacturonic acid in relation to xylose units generates short-chain molecules. It is amorphous in nature.

1.1.7 Lignin

Lignin, a complex molecule found in lignocellulosic biomass, contains several methoxy- and hydroxyl-groups that are conjugated in different ways. Lignin is primarily present in the outer layers of fibers, providing structural stiffness to the fibers. Its composition and structure vary depending on the variety of the biomass present and its abstraction process. The utilization of biomasses is promising for a variety of applications in the future.

Research Problem

The use of non-renewable resources for energy storage devices have many environmental disadvantages and their sources are depleting quickly. Developing highly efficient electrode

material from bio waste is a prerequisite for energy storage devices. The application of graphene-like carbon from bio waste for supercapacitors is an important development. Our research aims at synthesis of graphene-like carbon from olive pomace and date seed and its application in high performance supercapacitors.

Research Objectives

1. To Synthesize bio-waste derived graphene like carbon by thermo-chemical route
2. To achieve higher capacitive performance for super capacitor applications
3. To Characterize graphene and super capacitor electrode using different techniques such as SEM, XRD, FTIR, BET analyzer, Raman etc.

Chapter 2:

Literature Review

There are several methods available for transforming biowaste or residue into carbon-based compounds. Two main techniques i.e., carbonization and hydrothermal carbonization are employed to produce graphene-like carbon from biomass feedstocks for use as electrode material in supercapacitors.

Graphene-like carbon Synthesis

2.1.1 Carbonization

To eliminate volatile organic compounds such as CO₂, CO, or condensed liquids, a carbon-based substrate is subjected to high-temperature carbonization in the absence of air and the presence of an inert medium such as N₂ or argon. The carbonization process typically commences at around 300°C and varies depending on the feedstock. The main byproduct is small gas molecules, with pyrolysis converting 70% of the biomass into carbonaceous materials.

Figure 2-1 shows graphene type layered carbon produced from peanut shells waste [22]. The resulting powder underwent KOH activation being pyrolyzed in an Ar environment at 800 °C for 2 hours. Probe sonication with 10% H₂SO₄ and further activated powder took place for 1 hour. Potassium was utilized to cleave the graphene layers between the carbon atoms, while sonication was employed to accelerate the chemical activation by exfoliation process in an acidic environment. Both activation and sonication processes promote the separation of graphene sheets and enhance porosity, ultimately resulting in improved performance of supercapacitors.

The researchers aimed to produce graphene by utilizing activated carbon derived from various sources, such as walnut and almond shells, along with peanut shells. In comparison to peanut shell, the SSA of products made from walnut and almond shells was very low. According to their research, this is mostly because peanut shells exhibit a sheet-like structure, whereas walnut and almond shells aggregate extremely fragmented sheets. The sheet-like porous structure not only enhances ion transport and storage capacity but also promotes electrical conductivity through combining the effect of its highly accessible surface area. In an aqueous electrolyte of 1 M H₂SO₄, the PS-FLG displayed the highest energy and power density of 58.13 Wh/Kg and 37.5 kW/Kg respectively.

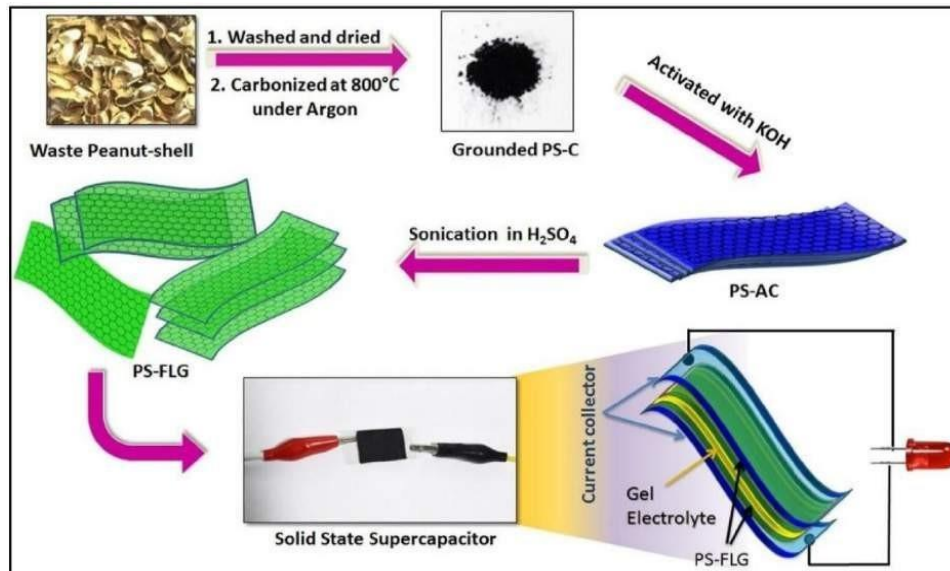


Figure 0-1 Synthesis representation of PS-FLG and its successive incorporation into a solid-state supercapacitor [23]

The electrochemical results support the statement mentioned earlier. Even when tested at a high scan rate of 1000 mV/s, the cyclic voltammetry (CV) curve maintained a rectangular shape with increased scan rate, indicating that pore size and electrical conductivity were in balance. Chemical activation with KOH was applied to rice husk to synthesize graphene by Sankar et al. [24] and Muramatsu et al. [25]. The process for creating graphene nanosheets from rice husk is shown in Figure 2-2. Instead of using an inert gas atmosphere like N₂ or Argon, an oxidative atmosphere was used to heat the ash. After activation with KOH, it was heated in air at 700°C for two hours, which led to the formation of black graphene nano powder. An ultrathin, wrinkled sheet-like material with SSA of roughly 1225 m²/g was seen in SEM pictures [24].

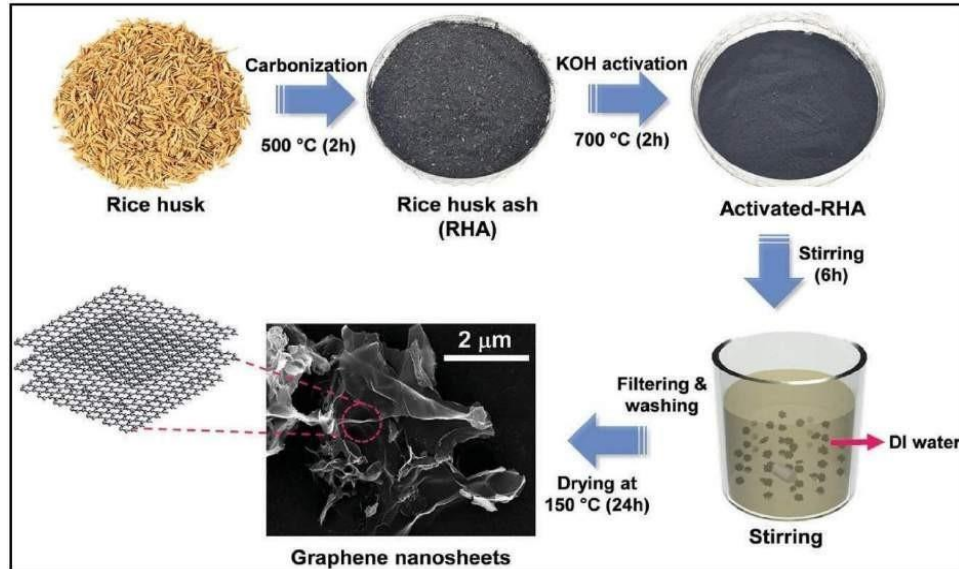


Figure 0-2 illustrates the process of producing graphene nanosheets using brown-rice husks as the source material [24]

2.1.2 Hydrothermal Carbonization

Hydrothermal carbonization (HTC) is a current area of focus in the synthesis of carbon-rich materials. This process can convert wet biomass into usable products [26]. Hydro char, which can be used as electrodes for energy storage applications, is produced through hydrothermal carbonization [27]. However, hydro char typically has a low specific surface area and poor porosity. It must then be activated or carbonized to change its chemical and physical characteristics [28]. Biodegradable waste or biomass can be effectively treated using hydrothermal treatment to create carbon-based products. Lu et al. [29] utilized lotus seedpods as a source of cellulose to produce a graphene-like structure. Cellulose, which is present in various layers of plants such as hemicellulose and lignin, has a crystalline structure that can be harnessed for this purpose. The lotus containers were chosen due to their porous structure and composition of polymeric cellulose. With the use of mild acids and oxidants, these cellulose units were oxidized and turned into sheets of nanocellulose. After carbonization, gas emerged because of the dissolution of bulky functional groups that inhibited carbon from aggregating and produced a characteristic structure when heteroatoms were added to the structure. The employment of an oxidant for pore development and a mild acid for exfoliation played the key roles in the production of porous activated carbon with properties resembling graphene nanosheets. Their synthesis was divided into three parts by Lu and his colleagues, only H_2O_2 or only HAc , or a

combination of H_2O_2 and HAc, were used in the hydrothermal process. Figure 2-3 depicts the process for creating activated carbon that resembles Graphene.

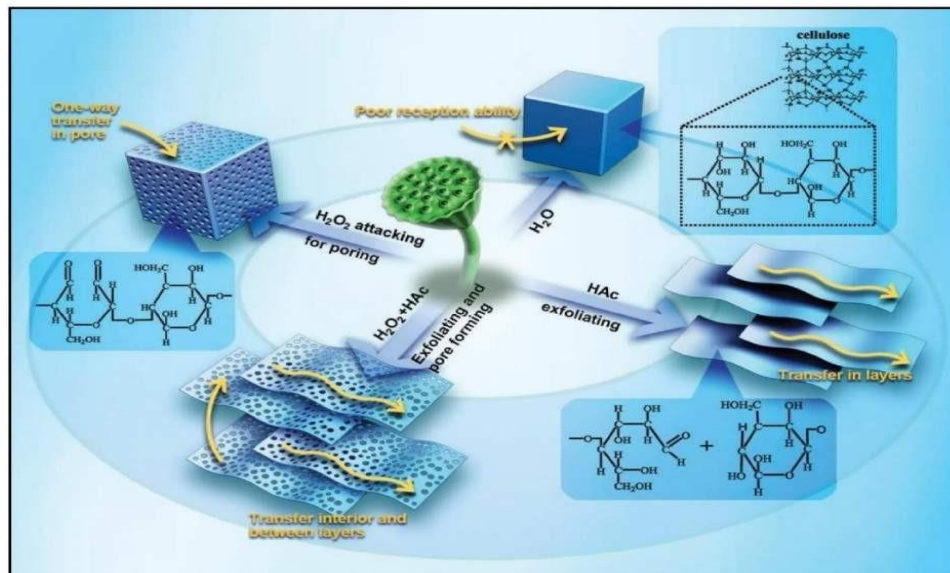


Figure 0-3 The synthesis mechanisms and methods for enhancing the electrochemical properties of graphene-like active carbon are illustrated in the figure, with arrows highlighting the ion transport pathways in C-H₂O, C-H₂O₂, C-HAc, and C-H₂O₂/HAc [28]

Chitosan has been utilized by several researchers, such as He et al. [30] and Primo et al. [31], as a biopolymer to create N-doped graphene films. Wang et al. [31] employed a cost-effective and straightforward spin coating method, followed by heating the nitrogen-containing chitosan films at 800°C in the presence of Ar gas flow. Nitrogen-doped Graphene was made using chitosan and acetic acid, and graphene films were made using an alginic acid and ammonia solution as a precursor. As a result, the hydro char produced during hydrothermal processing has a higher concentration of heteroatoms and serves as an excellent source for producing materials that are like Graphene and have adjustable functions and pore structures. The performance of various biomass sources used to create graphene-like structures is shown in table 2-1 along with their suitability as supercapacitors.

Table 0-1 Various lignocellulosic biomass feedstocks synthesize Graphene like carbon by carbonization method and their electrochemical performance for supercapacitors.

Biomass resources	Synthesis route	Electrolyte	Specific Capacitance (F/g)	Current density (A/g)	Stability	Ref.
Hemp	Hydrothermal carbonization with KOH as an activating agent	BMPYTFS I	142	100	96%,	[32]
Peanut shell	Carbonization conversion with chemical activation by KOH	1M. H ₂ SO ₄	186	0.5	87%,	[22]
Sugarcane bagasse	Hydrothermal carbonization synthesis with KOH activation	H ₂ SO ₄	280	1	90%,	[33]
Cornstalk	Carbonization followed by NaCl+KCL	1M.H ₂ SO ₄	407	1	92.6%	[34]
Poplar powder	Hydrothermal carbonization process with three activating agents (KOH, Urea & H ₂ O ₂)	6M KOH	508	1	95%	[35]
Spruce bark	Hydrothermal carbonization synthesis with KOH activation	6M KOH 1M TEABF ₄ /A N	398 239	0.5 1	96.3%	[36]
Cornstalk	Carbonization and activation by K ₄ [Fe(CN) ₆]	6M. KOH	213	1	98%	[34]

Chapter 3:

Methodology

Graphene-like carbon was synthesized from the waste biomass such as olive pomace and date seed. The procedure involves the thermochemical methods for graphene-like carbon synthesis

Synthesis of graphene-like carbon from olive pomace and date seed

3.1.1 Chemicals

- Potassium hydroxide (KOH)
- Hydrochloric acid (HCL)
- Distilled water

3.1.2 Procedure

Date seed (DS) was taken from the district DI khan, KPK, Pakistan and olive pomace (OP) was collected from the BARI Chakwal, Punjab, Pakistan. Potassium hydroxide (KOH), ethanol and hydrochloric acid (HCL) were purchased from Sigma Aldrich. For the synthesis of graphene-like carbon, DS was washed with distilled water and then dried at 90°C in the conventional drying oven for 12 hr. The dried sample were than crushed into fine particles of size 1mm by a grinder. Then, 3.0g of the finely grinded powder was taken with the 50ml of distilled water and was sealed into the 100ml Teflon-lined stainless steel autoclave, which was then heated at 180°C for 12hr in an electric oven. When it cools down and comes to the room temperature naturally, the resultant samples were collected out by the vacuum filtration with the help of filter paper, washed with the ethanol and deionized water many times and then dried in the conventional drying oven at 120°C for 12hr. The chemical activation than take place by mixing the carbonized precursor with KOH (Precursor / KOH 1:3) in a piston mortar. After that, the thoroughly grounded mixture was than calcinated at 800°C under the inert (N₂) atmosphere, at the heating rate of 10°C/min in the tube furnace. Subsequently, the activated obtained samples were than washed with 1M HCL solution and DI water, followed by the drying at 80°C for 12hr obtain graphene-like carbon.

The above mentioned process was applied again to obtain the graphene-like carbon from OP, only the starting precursor sample was changed.

Materials Characterization

3.1.3 Ultimate and proximate analysis

The proximate analysis of feedstock was performed, in accordance with the ASTM D176-84 standards, to obtain the fixed carbon, volatile matter, moisture and ash content. Elemental analysis of both feedstock and as-prepared carbon samples was performed using the CHN-elemental analyzer (model SE-CHN200) to find C, H, N and O content.

3.1.4 XRD

X-ray diffraction pattern was recorded from the X-ray diffractometer (XRD) using 2D phaser.

3.1.5 SEM

Structures and morphologies of the as-prepared carbon samples was characterized by the Scanning electron microscopy (SEM, JEOL-JSM-6490LA).

3.1.6 EDX

Elemental composition was determined by the Energy dispersive x-ray analysis using EDX Z2-i7 detector attached to the SEM.

3.1.7 Raman spectroscopy

To study the degree of graphitization and detects in morphology, Raman spectra was obtained from the Raman spectrophotometer (BWS415-532S- i Raman).

3.1.8 FTIR

To obtain the chemical composition, FTIR was performed under the frequency range of 400-4000cm⁻¹ by using the FTIR spectroscopy.

Electrodes Preparation

Electrode preparation contained ink formation, treatment of support material and deposition of ink on its surface.

Ink Formation

1. Ink was prepared by mixing 85 % of active catalyst, 10 % carbon black (conductive additive), 5 % Polyethylene difluoride (PVDF) as binder, and 0.4 ml 1-methyl-2-pyrrolidone (NMP) as solvent.
2. Mixture was sonicated for 3 h.

Support Material Treatment

3. Nickel foam served as conductive support material. $1 \times 1 \text{ cm}^2$ Ni foam was cut.
4. It was treated by 30 min sonication in 2M HCL and ethanol each.
5. It was dried at 60 °C for 1 h.

Ink Deposition

6. The prepared ink was deposited on treated Ni foam to form electrode.
7. Electrode was dried at 80 °C for 24 h.
8. Two electrodes were prepared: DS 800 & OP 800 by following the same procedure.

Electrochemical Testing

Gammry is the research-grade potentiostat present at SCME. Equipment consists of workstation, electrochemical cell, computer hardware, and software system. It is used for many applications including

- Battery testing
- Fuel cell and biofuel cell
- Liquid conductivity
- Electrochemical deposition of thin film
- Material impedance spectroscopy,
- Corrosion testing
- Photovoltaics and sensors

Capacitor and supercapacitor testing Supercapacitor testing was performed on potentiostat.

Chapter 4:

Results & Discussion

The synthesized materials were characterized using XRD, SEM, EDX and BET. XRD determined the crystal structure and particle size. SEM and EDX were used to determine surface morphology and elemental composition. FTIR was applied to study the presence of functional groups.

Electrochemical testing was performed to evaluate CV curves, GCD curves, electrochemical resistance and cyclic stability of electrode material.

Physicochemical Characterization

Figure 4-1 shows the schematic diagram for the synthesis of graphene-like carbon from olive pomace (OP) and date seed (DS). Figure 4-2(a) shows the proximate analysis of OP and DS on the dry basis. It shows that the OP contain moisture content upto 2%, volatile matter 75.7%, fixed carbon 18.2% and ash upto 5.2%. Whereas, the DS contains moisture content 10.2%, volatile matter 34.16%, fixed carbon 44.3% and ash upto 1.34%, respectively. By having high fixed carbon and volatile matter, these precursors were considered suitable for the synthesis of graphene-like carbon. These factors are the important elements to support their suitability [37]. Figure 4-2(b) indicates the ultimate analysis of OP, OP 900, DS and DS 800. It shows that the OP and DS contains carbon content of 50.9% & 44.84, respectively, with very less amount of hydrogen and nitrogen. Oxygen content in OP and DS are 35.8% and 40.94%, respectively. When OP and DS were subjected to the chemical activation at 800°C, the synthesized graphene-like carbon samples contained high carbon content of 68.1% and 57.8%, respectively. A higher carbon content in as-prepared samples as a result of the strong oxidizing and dehydration actions of sulfuric acid and high activation temperature caused the volatilization of the other compounds.

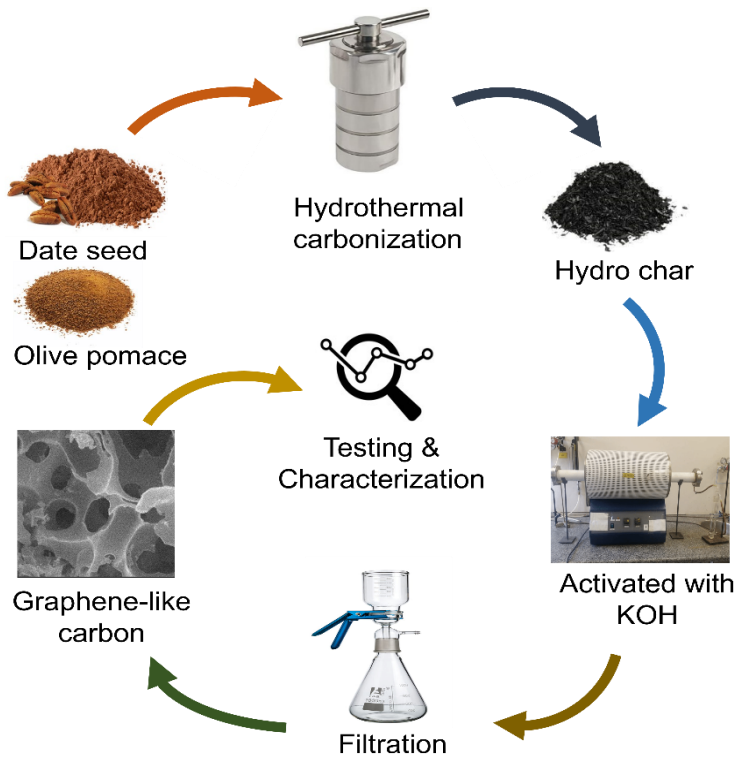


Figure 0-1 Schematic diagram for synthesis of graphene-like carbon

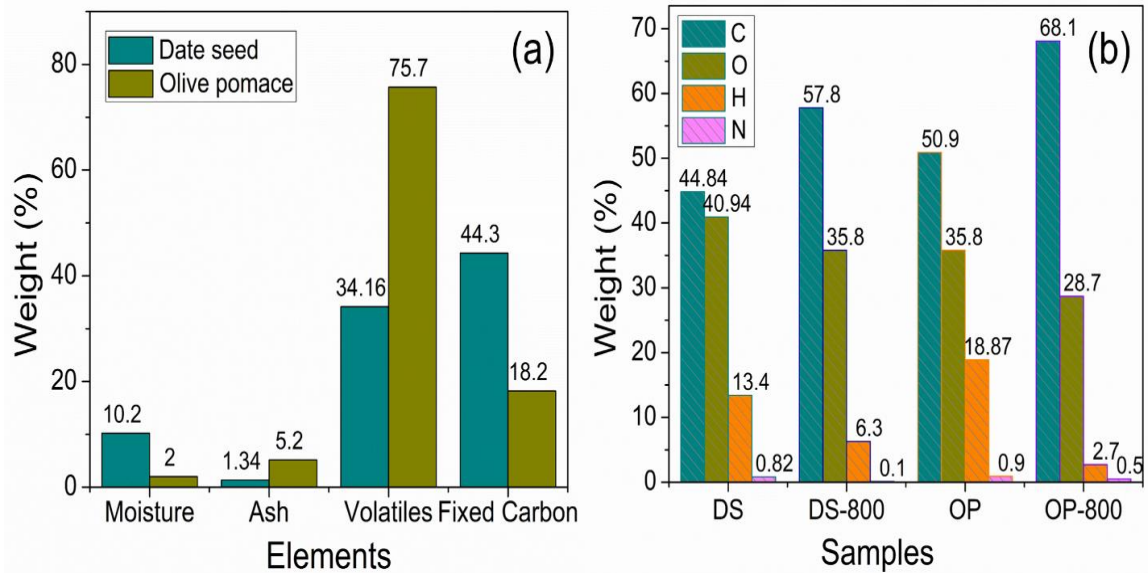


Figure 0-2 (a) Proximate analysis of OP and DS, (b) Ultimate analysis of DS, DS-800, OP, OP-800

4.1.1 XRD

Figure 4-3 exhibits the XRD analysis that indicates the amorphous and crystalline nature of as prepared samples. There was no sharp peak observed for DS 800 which indicates its less crystalline nature as compared to the OP 800. However, for OP 800, a sharp graphitic peak was observed at $20 \approx 23^\circ$ (002) and 43° (001) planes, indicating the presence of graphene sheets[38]. The peak at (002) plane is much sharper and broader than the peak at (001) plane attributed to the (100) plane of distorted graphitic sheets, which indicates the high degree of crystallinity of the OP 800 [39]. Peaks at these scattering angle ranges often result from (002) diffraction, which is caused by stacking of graphene sheets, whereas a very small peak at 43° is caused by (101) diffraction, which is caused by the existence of small realms of ordered graphene sheets [40]. These diffractograms demonstrate that KOH itself, through chemical reaction and potassium ion release, plays a significant part in the intercalation of graphitic carbon into graphene sheets [41, 42].

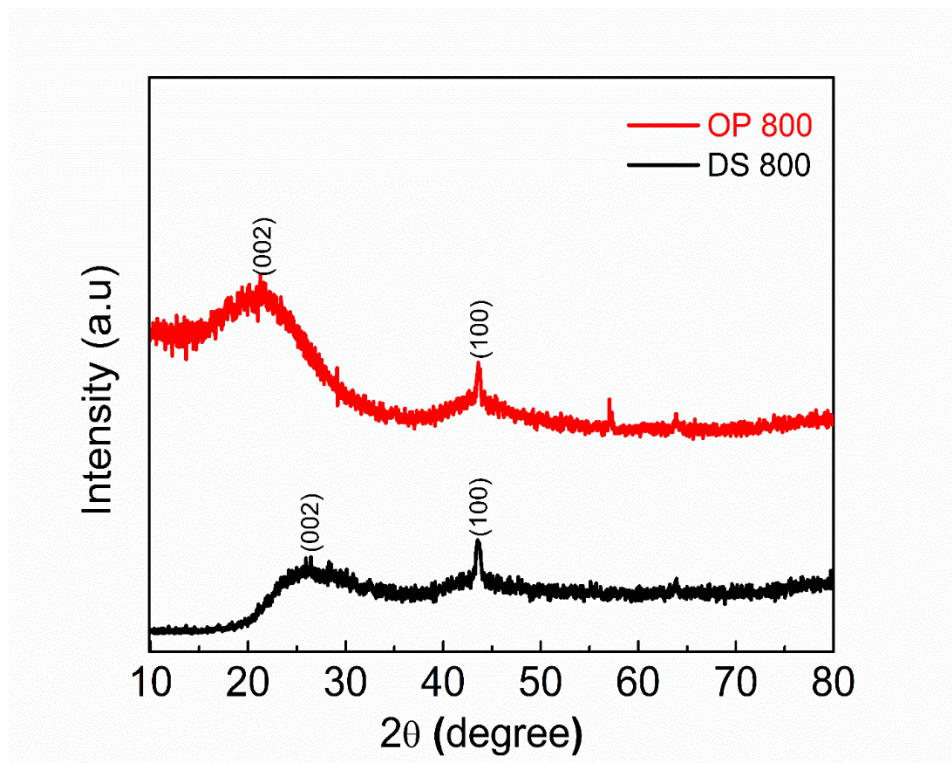


Figure 0-3 XRD pattern of OP 800 and DS 800

4.1.2 Raman spectroscopy

The phase structure of the as-prepared was also investigated using Raman spectra. Two prominent peaks can be seen at 1348 cm^{-1} (D-band) and 1591 cm^{-1} (G-band), as illustrated in Figure 4-4. The OP 800 shows the I_D/I_G ratio of 0.82, indicating good degree of graphitization and an ordered structure. The pattern of the OP 800, in contrast, show a characteristics peak, which indicates the graphitization of carbon materials. In general, the few-layered, well-graphitized graphene is found in the strong 2D peak without the usual graphite hump [43]. The modest D peaks of DS 800, which are signs of few flaws in the graphene, also point to the good quality of the few-layered graphene.

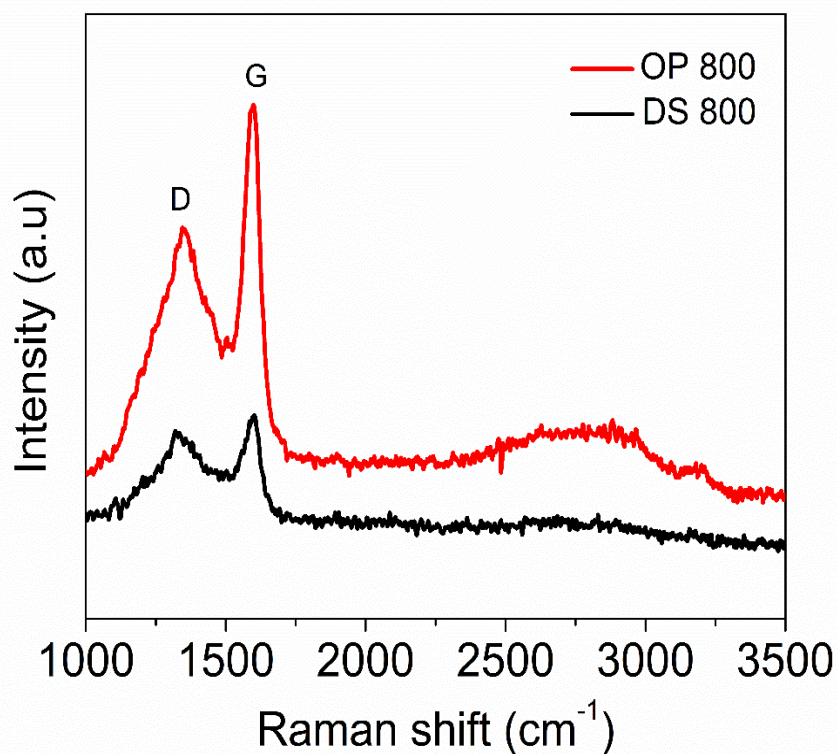


Figure 0-4 Raman spectra of OP 800 and DS 800

4.1.3 FTIR

The presence of functional group in the as prepared samples was analyzed by the Fourier transform infra-red (FTIR), as shown in figure 4-5. FTIR spectrum was recorded under the range of 400-4000 cm^{-1} . An absorption peak was observed at 3400-3500 cm^{-1} ; which point outs the stretching of $-\text{OH}$ bond present in the carbon samples [44]. The peaks observed at the range of 2800-3000 cm^{-1} indicates the presence of $-\text{C}-\text{H}$ bond. At 1630 cm^{-1} , graphene-like sheets showed skeletal ring vibration [45], which is more prominent in OP 800. The presence of peaks between 1500-1600 cm^{-1} also indicates the presence of $-\text{C}=\text{C}$ [46]. Furthermore, peaks between 1250-1053.53 cm^{-1} indicates the presence of $-\text{C}-\text{O}$ functional group, which are present in cellulose and hemi-cellulose [47]. However, no peak was observed between the range of 1250-1053.53 cm^{-1} for OP-800, which indicates the absence of $-\text{C}-\text{O}$ bond, showing the complete degradation of cellulose and hemi-cellulose at high temperature.

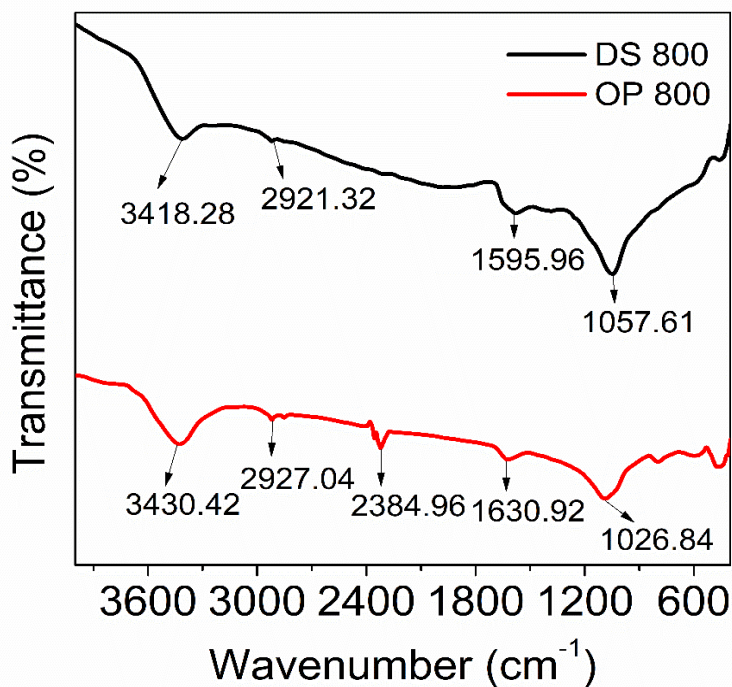


Figure 0-5 FTIR analysis of OP 800 & DS 800

4.1.4 SEM

Figure 4-6(a & c) shows the particles of OP and DS precursor before chemical activation, as it shows that both precursor contain less porosity and clogging of pores. Whereas, Figure 4-6 (b & d) shows the surface morphology of OP and DS derived graphene-like carbon. It shows that high ratio of KOH leads to the more porous structure and activation at the high temperature also caused to increase the porosity. The as prepared samples exhibit three dimensional structure at the activation temperature. Among the OP 800 & DS 800, OP 800 exhibits an ordered 3D structure with more porous structure and high porosity, as shown in figure 4-6 (b). It also indicates the presence of meso and macro pores across the surface of graphene-like carbon. KOH can more efficiently exfoliate the carbonized precursor's multilayered structure into graphene like carbon at high temperature. According to earlier studies, the combination of macro- and meso-pores offers plenty of area for charge storage, and pathways for quick charge transfer, electrolyte penetration, improving supercapacitor performance [48].

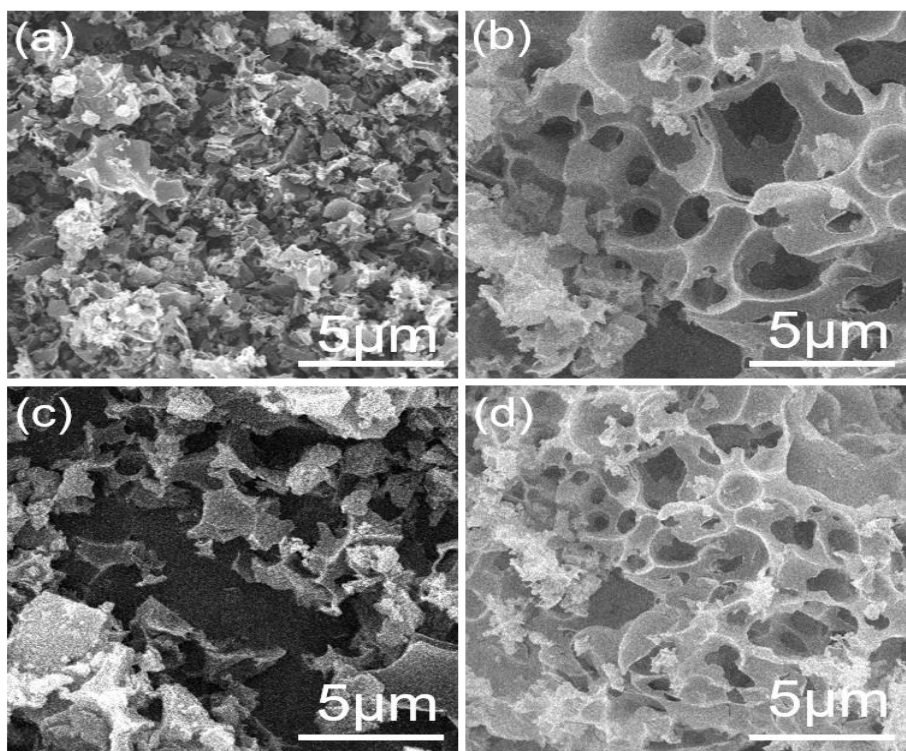


Figure 0-6 (a & c) SEM images of precursor OP and DS. (b) SEM image for synthesized graphene-like carbon from OP at 800°C (c) SEM image for synthesized graphene-like carbon from DS at 800°C

4.1.5 EDX

Figure 4-7 shows the EDX analysis of samples. C and O were found to be the main chemical components of these as prepared samples. Figure 4-7 (a) the EDX analysis of raw DS, which contains the 55% C and O content of 44%. Figure 4-7 (b) shows the chemical composition of DS 800. After the chemical activation at 800°C, DS 800 contains the carbon content of 83.6% and contain less oxygen of 16.4%. Figure 4-7 (c) exhibits the EDX analysis of raw OP which contain C & O content of 58.1 and 40.9%, respectively. However, OP 800 contain the highest C content of 92.3% with very less oxygen content of 7.7%, as shown in figure 4-7 (d). EDX analysis and raman spectroscopy confirms the high degree of graphitization with less disordered structure of OP 800, with the presence of few oxygen functional groups, as compared to the other samples. These functional groups increase the pseudocapacitive behavior by involving in the faradic reactions, which results in better electrochemical performance.

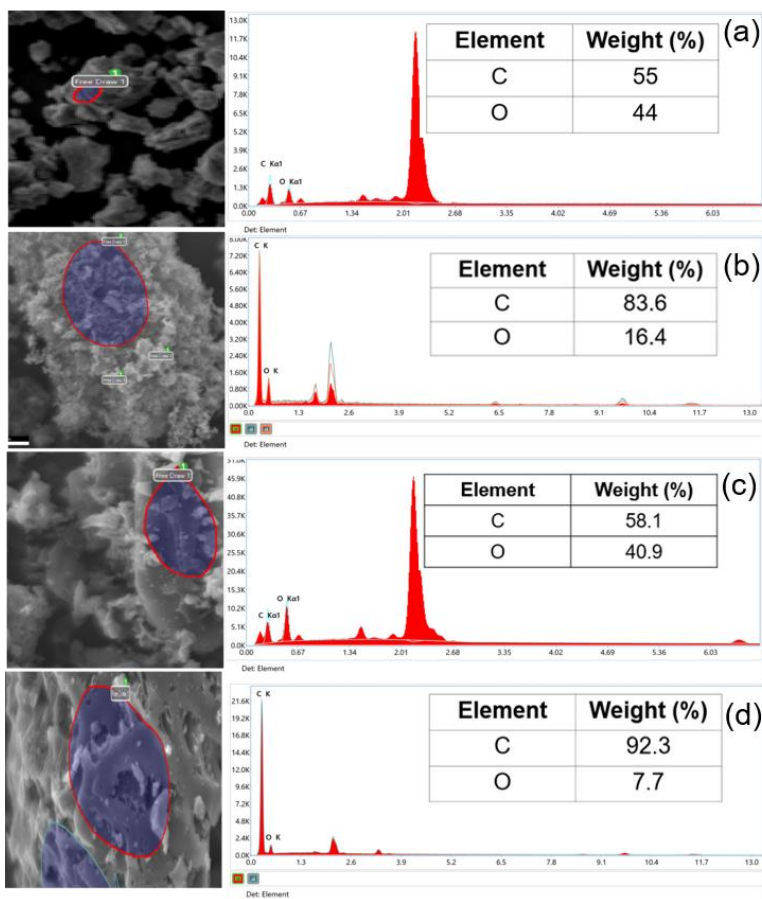


Figure 0-7 EDX analysis of samples (a & c) EDX analysis of raw DS and OP (b) exhibits the EDX composition of DS 800 (d) EDX of OP 800

Electrochemical Testing Results

4.1.6 Three cell electrode testing

4.1.6.1 CV Curves

The electrochemical performance analysis of as prepared samples OP 800 and DS800 was firstly performed in three cell electrode system using 1M electrolyte solution. Figure 4-8(a) shows the Electrochemical performance of OP 800 through a cyclic voltammogram. Different scan rates were chosen for both samples and performed cyclic voltammetry at 10, 30, 50 and 100mV/s respectively, at lower scan rates both samples gave similar behavior but at higher scan rates at 100 mV/s. Figure 4-8(b) clear difference can be seen in OP 800 compared to DS 800, giving more prominent oxidative peaks and higher capacitance. The cyclic voltammogram obtained at 100 mV/s exhibits an asymmetric shape, indicative of a mixed charge storage mechanism. OP 800 shows more capacitance and pseudocapacitive behavior compared to DS 800. The sharp oxidative peak observed at 0.5 V suggests fast and reversible redox reactions during the forward scan, indicating pseudocapacitive contribution. Conversely, the less sharp reduction peak observed at -0.002 V signifies slower and partially reversible redox reactions during the reverse scan.

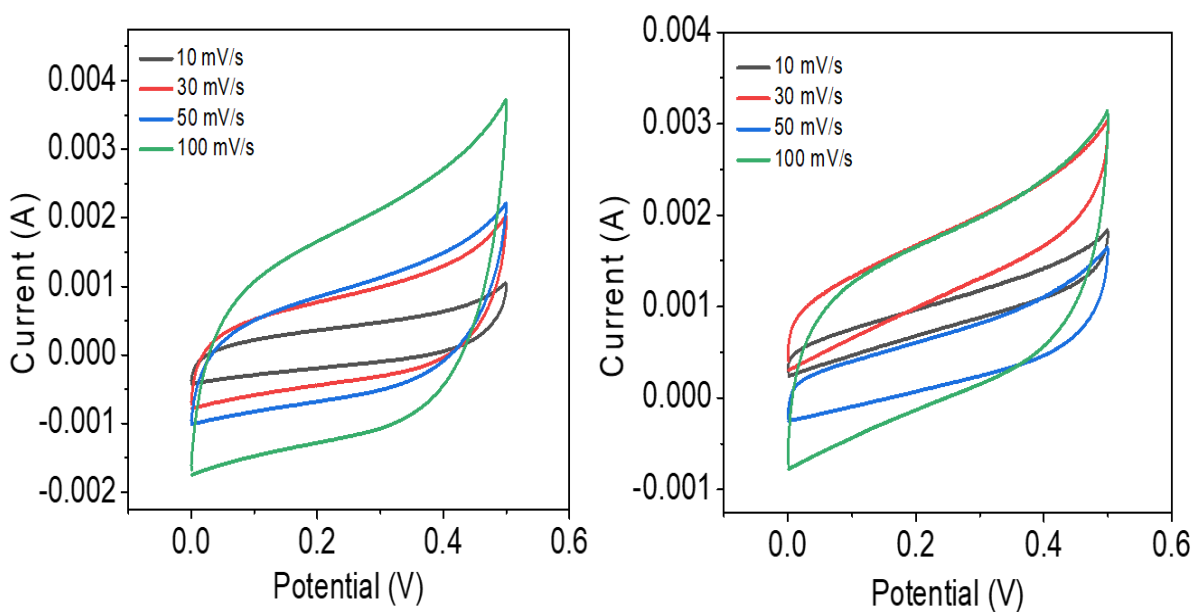


Figure 0-8 (a) CV curves of OP 800 at different scan rates (b) CV curves of DS 800 at different scan rates

Figure 4-9 summarizes the comparison of two samples which supports OP 800 sample as high oxidative peak giving sample. The slight rectangular shape in between reflects the electrical double-layer capacitor (EDLC) behavior, signifying physical adsorption of ions. At lower scan rates the current is modest, and a CV curve demonstrates a more or less rectangular shape, indicative of a capacitive-dominated charge storage mechanism (EDLC). At slow scan rates, sufficient time allows for the generation of a consistent electric double layer at the electrode/electrolyte interface, contributing to more capacitive behavior, as the scan rate increases, the response of the current becomes more prominent by transforming the CV curve. The change of rectangular like shape to more peaked appearance, indicating a transition from capacitance dominance to faradaic processes. This combined behavior of pseudocapacitive and EDLC characteristics enhances energy storage capacity and charge-discharge rates, making the material promising for high-performance supercapacitor applications.

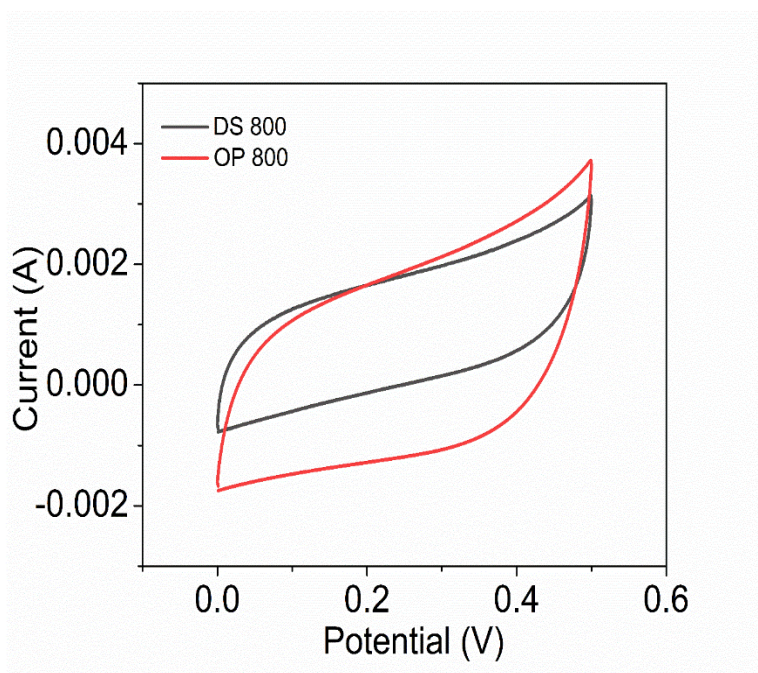


Figure 0-9 Comparison of CV curves of OP 800 and DS 800 at the scan rate of 100 mV/s

4.1.6.2 GCD curves

Figure 4-10(a) presents a Galvanostatic charge-discharge (GCD) curve obtained for OP 800 at different densities of current (0.5, 1, 2 and 5 A/g). Curve shows a non-linear behavior due to the involvement of faradaic reactions and pseudo capacitance occurring during charge and discharge. Faradaic reactions involve the transfer of electrons during the electrochemical reactions,

resulting in the reversible oxidation and reduction of species at the electrode interface. Pseudocapacitive behavior is usually observable when there are some hydroxides which results in rapid non-linear charge storage. Figure 4-10(b) depicts a plot of DS 800 at same conditions and exhibits almost similar trend of a mix of EDLC and pseudocapacitive behavior like OP 800. Furthermore, non-homogeneity, ion diffusion and complexity of electrode-electrolyte interface also contributes such behavior.

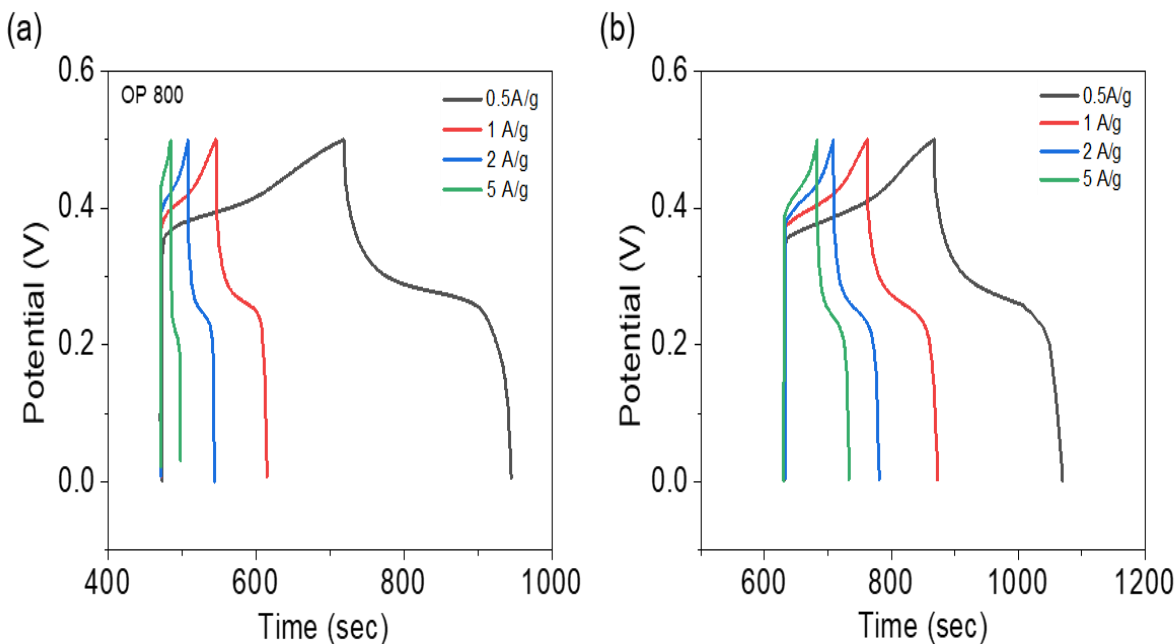


Figure 0-10 GCD curves of OP 800 at different current densities (b) GCD curves of DS 800 at different current densities

Figure 4-11 presents a comparative analysis of GCD curves for OP 800 and DS 800 electrodes. The combined curve vividly illustrates the significant discrepancy in discharge times between the two samples, providing compelling evidence of OP's superior electrochemical performance over DS. Moreover, Specific capacitance is measured at varying current densities figure 4-12(a) for both samples showed a notable sensitivity to applied current density. At lower current density of 0.5 Ag^{-1} OP 800 displays more specific capacitance, indicating a gradual and slower charge discharge process compared to DS 800. Conversely at higher current densities of 2 and 5 Ag^{-1} , GCD depicts faster charge and discharge cycles.

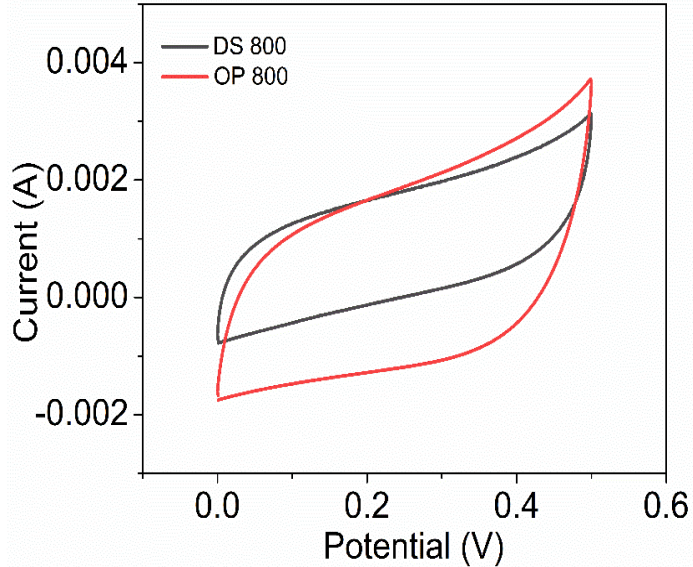


Figure 0-11 GCD curves of OP 800 and DS 800 at the current density of 0.5 A/g

After calculating the specific capacitance, the results reveal that the olive pomace manifests a remarkable capacitance of 502 F/g, at 0.5 A/g differing from DS 800 which shows 460 A/g. At higher currents of 1, 2 and 5 A/g the capacitive performance decreases linearly but OP 800 is behaving better in terms of retaining its performance. specific capacitance of Olive Pomace tested is much better than the previously reported biomass samples like soya bean derived porous carbon structure exhibited a capacitive performance of 276 F/g at a current density of 0.5 A/g [49], while Spruce bark carbon nanosheets displayed a value of 305 F/g at a current density of 0.2 A/g [50] and corn husk derived porous carbon demonstrated a capacitive performance of 260 F/g at 1 A/g [51]. OP 800 manifests better results probably due to its high surface area, greater existence of oxygen functional groups, like hydroxyl (-OH) and carboxyl group(-COOH) [52], and high amount of lignin, cellulose, and hemicellulose. More presence of functional groups creates excess active sites for charge storage and promotes pseudocapacitive.

4.1.6.3 EIS

Electrochemical Impedance Spectroscopy (EIS) was employed to assess the Ion transport characteristics within two different electrodes as shown in figure 4-12(b). The presence of a 45° linear line in low frequency region clearly indicates the existence of Warburg impedance. It basically shows that the Ion transport processes in the electrode material are diffusion limited,

and the charge transfer rate is stabilized by the movement of ions or charge carriers in the electrolyte towards the electrode surface. The slope also gives insights into the coefficient of Warburg and ions mass transport.

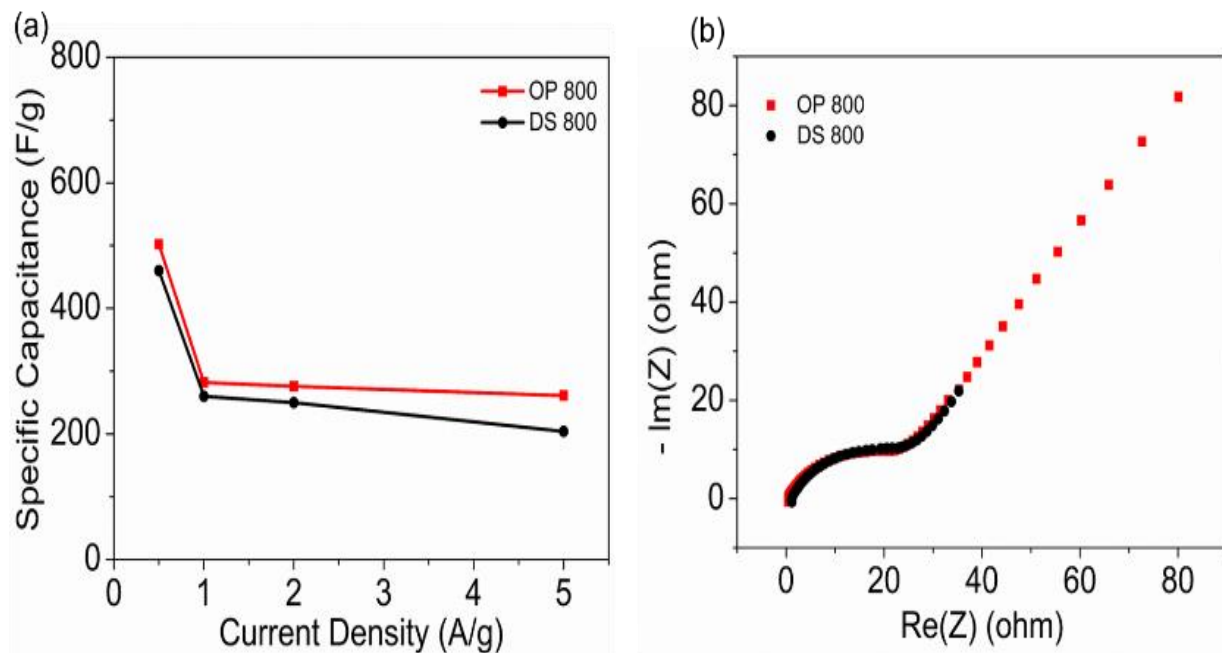


Figure 0-12 (a) Specific capacitance of OP 800 & DS 800 at different current densities (b) Nyquist plot for as-prepared materials

The semi-circle can be seen at the Intermediate frequencies in the Nyquist plot depicts a combination of a capacitive and faradaic processes. The capacitive component of the impedance is represented by the diameter of the semi-circle, indicating the electrical double capacitance (EDLC) behavior. The faradaic processes, which involve redox reactions or other chemical interactions at the electrode-electrolyte interface, contribute to the curvature of the semi-circle.

The higher frequency region in the EIS graph follows a line with an x-intercept, this represents the equivalent series resistance (ESR). ESR amalgamates the resistance from the electrolyte, internal resistance from the active components, substrate, and collector contact resistance [53-55]. A lower ESR shows better ion transport and improved overall electrode performance. The calculated ESR in this paper is 0.47Ω for OP 800 sample, as shown in [table 4-1](#), which is quite low compared to the previously reported biomass samples [50, 56, 57]. The use of Nickel foam compared to glassy carbon leads to a better ESR as Nickel foam has high conductivity and porosity which facilitates efficient ion transport.

Table 0-1 ERS and RCT vales of as prepared samples of OP 800 & DS 800

SAMPLE	RS (OHM)	RCT (OHM)
OP 800	0.47	22.9
DS 800	0.67	23.3

4.1.7 Two cell electrode testing

4.1.7.1 CV curves

The two-cell electrode testing was performed for the OP 800 sample to validate its electrochemical performance in aqueous KOH solution. Figure 4-13 shows CV curve of OP 800 sample at varying scan rates of 10, 50 and 100 mV/s in a voltage range of -0.5 V to 0.5V. The observed pattern indicates a dynamic interplay between the behavior of Electrochemical Double layer capacitor (EDLC) and faradaic processes. The clear sharpening of peak at higher scan rates of 100 mV/s suggests faradaic responses means fast and reversible redox reactions, which was also observed in three cell testing. With the increase in scan rate at 100 mV/s the curve depicts more positive current and sharp peaks.

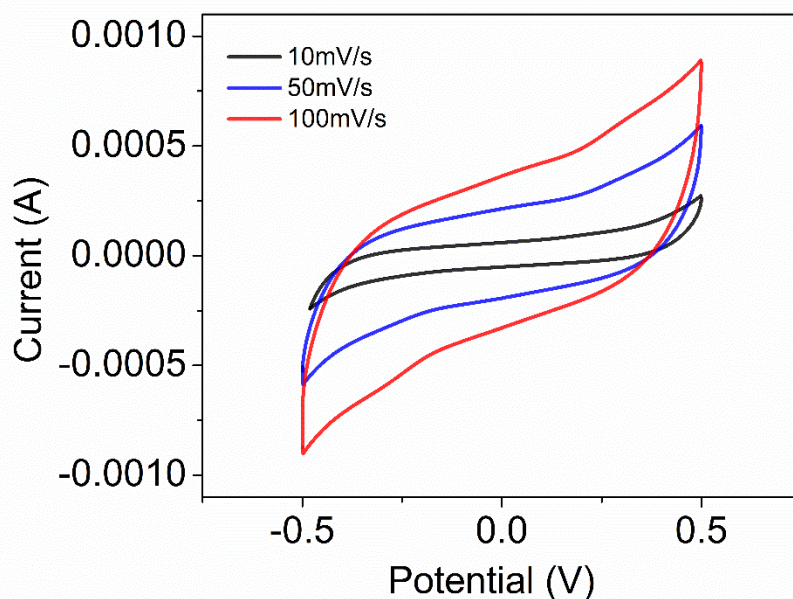


Figure 0-13 CV curves of OP 800 at different scan rates

4.1.7.2 GCD curves

Figure 4-14 shows the GCD curve of OP 800 sample which is quite consistent with the previous measurements with three cell electrode. GCD curve clearly shows the voltage drop occurring at just the start of discharge curve. The non-linearity of the graph validates that the charge storage mechanism is mainly due to the oxidation and reduction reactions. The impact of voltage drop caused by resistance (IR) on energy delivery is extremely important. When the internal resistance

is higher there are more energy losses. Within the context of Figure 4-14 inset, a correlation between voltage drops and current density is apparent. While the relationship demonstrates an overall linear trend, the presence of deviations from linearity underscores the subtle mix of different factors affecting the voltage drop. Notably, during the charge-discharge process, electrolyte ions traverse from solution to the electrode's internal pore surface. The intricate dynamics of ion transport, particularly within the pore structure and diameter, contribute to the observed deviations from a perfectly linear relationship [49].

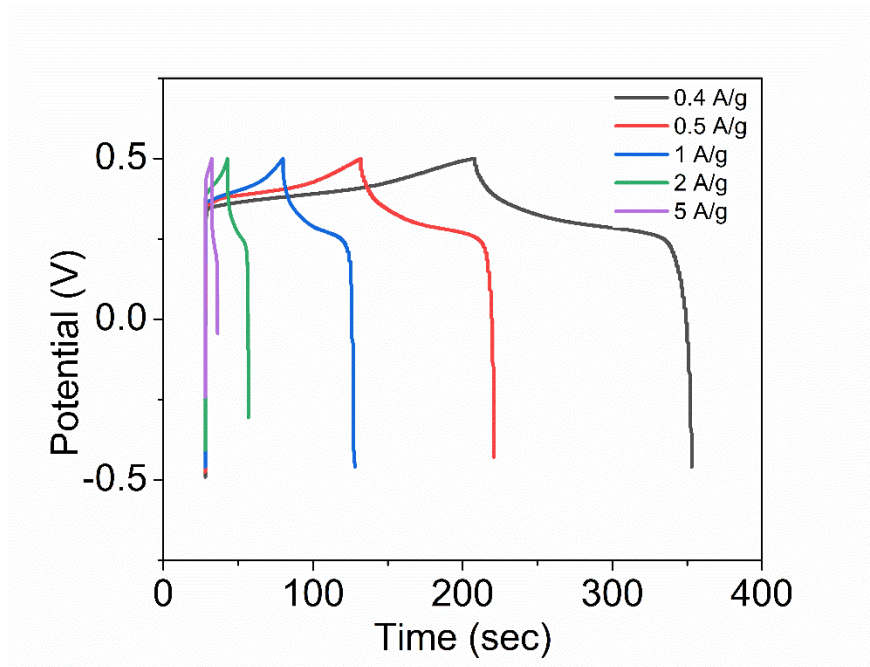


Figure 0-14 GCD curves of OP 800 at different scan rates

4.1.7.3 Specific capacitance vs current density

Figure 4-15 shows a specific capacitance of OP 800. Specific capacitance of 518 F/g is observed at a current density of 0.4A/g which is much higher than the previously reported samples, as shown in table 4-2. The capacitive performance gets lower usually at very high current densities of 5A/g.

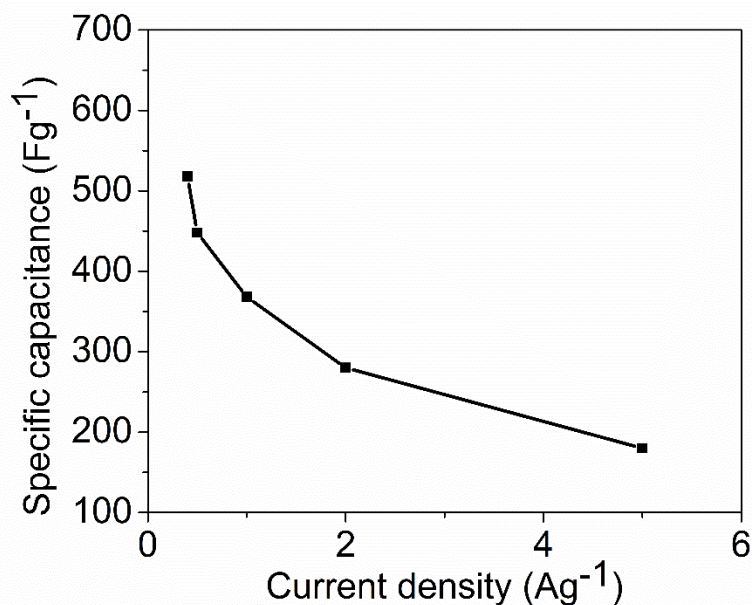


Figure 0-15 Specific capacitance of OP 800 at different current densities

4.1.7.4 Energy density vs power density

Figure 4-16 depicts the Ragone plot of OP 800 derived supercapacitor in 1M KOH solution. At the mentioned Power density of 450 W/kg the olive Pomace sample gave the maximum energy density of 53 Wh/kg, which is quite greater than in the afore-mentioned literature [58-60].

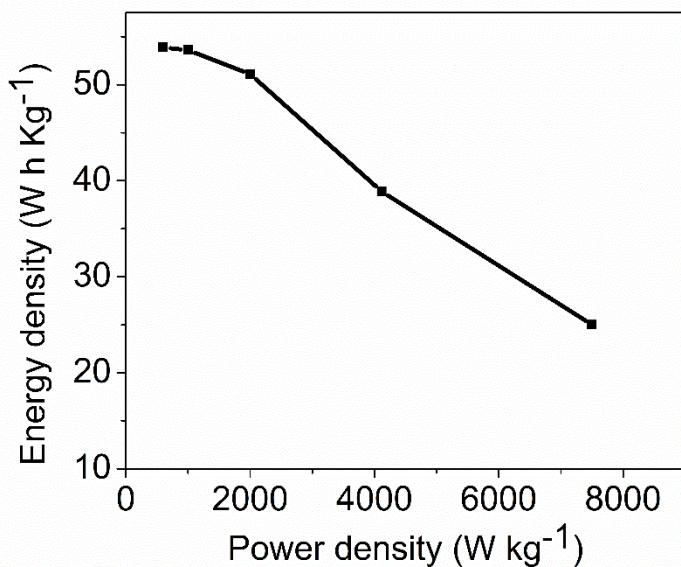


Figure 0-16 Ragone plot for as-prepared symmetric supercapacitor

4.1.7.5 EIS

Figure 4-17 depicts a EIS graph of OP 800 sample which was performed after 1000 cycles of stability. It's worth noting that the resistance only increased slightly to 0.57Ω which is actually an indication of good performance of OP and can be regarded a trusted material for use as an electrode.

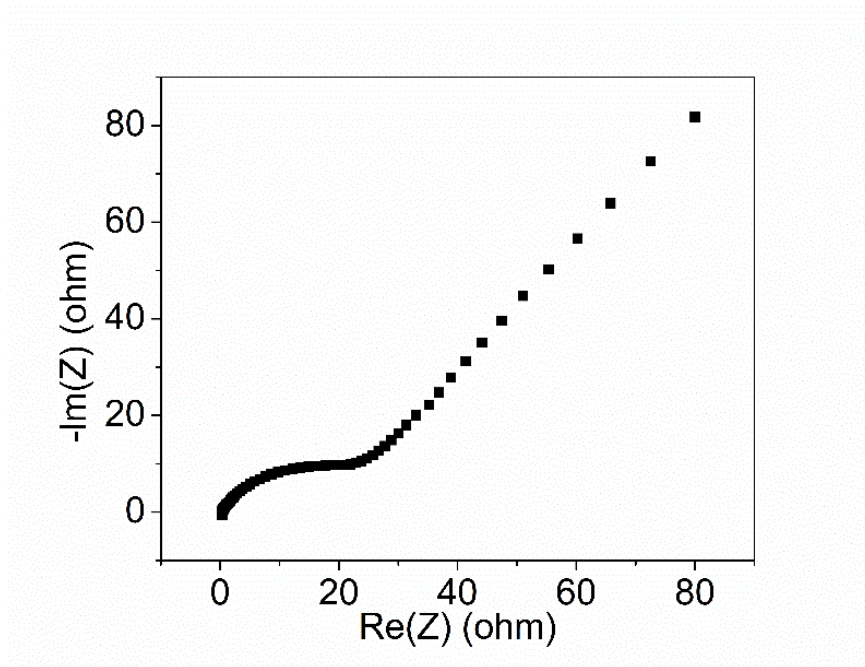


Figure 0-17 Nyquist plot for OP 800

4.1.7.6 Cyclic stability

Figure 4-18 shows the good electrochemical performance by OP in terms of its reversibility and stability over repeated cycles. After 1000 cycles at the current density of 5 A/g , OP gives 96% retention which confirms its ability as a supercapacitor.

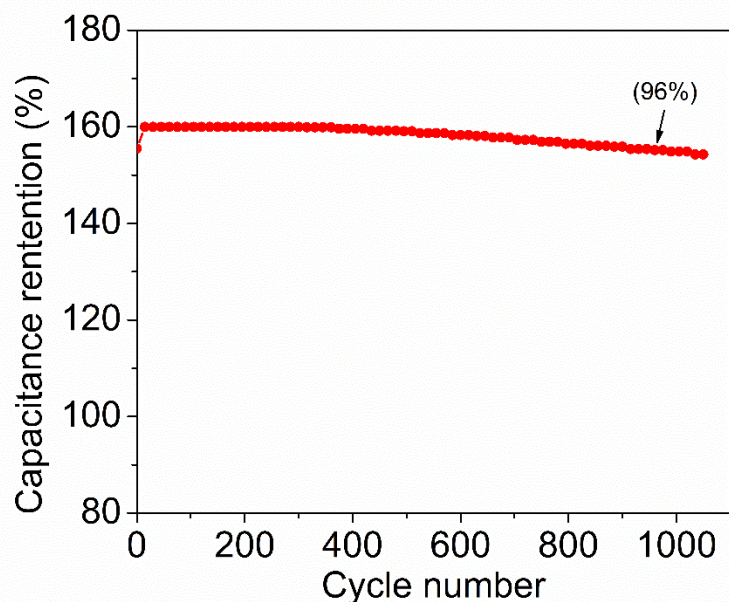


Figure 0-18 Capacitance retention of OP 800 in IM electrolyte after 1000 cycles at 5 A/g

The experimental results highlight Olive Pomace impressive performs well in the aqueous electrolyte. To optimize performance, the pore size must align with electrolyte ion dimensions. Aqueous electrolyte ions, being smaller than 1 nm, can access micropores (< 2 nm) for efficient double layer formation. Organic electrolytes, however, face challenges due to restricted ion access and inefficient micropore utilization, hampering capacitive performance. By introducing mesopores (2–50 nm), porous carbon enhances surface area utilization and mass transfer, favoring power density [61, 62]. All these results favor the OP 800 as an electrode material for good electrochemical performances in organic electrolytes.

Table 0-2 Electrochemical performance of activated carbon synthesized from different biomass feedstocks via carbonization and hydrothermal carbonization

Biomass	Preparation method	Electrolyte	Current density (A/g)	Specific capacitance (F/g)	Ref
Peanut shell	Carbonization conversion with chemical activation by KOH	1M. H ₂ SO ₄	0.5	186	[23]
Pear	Hydrothermal carbonization with KOH as an activating agent	1M TEAB4/AN	2	126	[63]
Coconut shell	Carbonization and chemical activation using FeCl ₂ as an activation agent	6M. KOH	1	276	[64]
Sugarcane bagasse	Hydrothermal carbonization synthesis with KOH activation	1M. H ₂ SO ₄	1	280	[65]
Spruce bark	Hydrothermal carbonization synthesis with KOH activation	6M KOH	0.5	398	[50]
Cornstalk	Carbonization followed by NaCl+KCL activation	1M. H ₂ SO ₄	1	407	[66]
Tamarisk roots	Carbonization conversion and chemical activation by zinc chloride & sodium chloride	2M. KOH	0.5	293	[67]
Poplar powder	Hydrothermal carbonization process with three activating agents (KOH, Urea & H ₂ O ₂)	6M KOH	1	508	[68]
Olive pomace	Hydrothermal carbonization with KOH activation	1 M KOH	0.4	518	This work

Conclusion

In summary, the above study from three cell electrode testing revealed that the graphene like carbon derived from olive pomace gives better electrochemical performance as compared to graphene-like carbon from date seed. The as-resulted OP 800 gives specific capacitance of 51 Fg^{-1} at the current density of 0.4 A/g in two cell electrode testing, due to its well-ordered 2D structure and presence of macropores and mesopores, as shown in the SEM images. Additionally, the formation of nanosheets adjacent to the pores serves as the ion absorbers and provides access to the inner surface, which accelerate the transfer of ions by lowering the electric resistance, thus making the graphene like carbon suitable for electrochemical energy storage devices. The low I_d/I_g ratio for OP 800 shows the highly ordered graphitic structure, which enhances the electrolytic ion diffusion and conductivity, resulting in high electrochemical performance. Moreover, the synthesis of graphene-like carbon from biomass like OP & DS which are abundant, environment friendly, economical, makes these raw material suitable candidates as clean energy sources and making them a potential candidate for supercapacitors. This work offers an easy and reliable method the for graphene-like carbon synthesis from renewable waste biomass, and their application as electrode material for supercapacitors. Moreover, the structural configuration of OP 800 with inherited properties of graphene, makes it a potential candidate as clean energy source for energy storage and conversion devices.

Recommendations

1. Further research is necessary to gain a comprehensive understanding of both the macroscopic and microscopic processes that occur during carbonization and hydrothermal carbonization. Such investigations are essential to enhance the performance of materials containing graphene-like carbon linings, particularly in supercapacitor applications.
2. To address the issue of graphene layers restacking, it is crucial to prioritize the comprehensive synthesis of crumpled and porous graphene with holes on sheets, along with investigating their potential applications.
3. For prospects in energy storage applications such as SCs, a techno-economic examination of the synthesis of materials similar to graphene using carbonization and hydrothermal carbon methods is also required.

References

- [1] D. Gielen, F. Boshell, D. Saygin, M. D. Bazilian, N. Wagner, and R. Gorini, "The role of renewable energy in the global energy transformation," *Energy Strategy Reviews*, vol. 24, pp. 38-50, 2019/04/01/ 2019.
- [2] S. T. Glassmeyer *et al.*, "Nationwide reconnaissance of contaminants of emerging concern in source and treated drinking waters of the United States," *Science of The Total Environment*, vol. 581-582, pp. 909-922, 2017/03/01/ 2017.
- [3] C. Fraiture, M. Giordano, and Y. Liao, "Biofuels and implications for agricultural water use: Blue impacts of green energy," *Water Policy*, vol. 10, 02/01 2008.
- [4] K. Zhu, Y. Sun, R. Wang, Z. Shan, and K. Liu, "Fast synthesis of uniform mesoporous titania submicrospheres with high tap densities for high-volumetric performance Li-ion batteries," *Science China Materials*, vol. 60, 02/06 2017.
- [5] E. E. Miller, Y. Hua, and F. H. J. J. o. E. S. Tezel, "Materials for energy storage: Review of electrode materials and methods of increasing capacitance for supercapacitors," 2018.
- [6] A. González, E. Goikolea, J. A. Barrena, and R. Mysyk, "Review on supercapacitors: Technologies and materials," *Renewable and Sustainable Energy Reviews*, vol. 58, pp. 1189-1206, 05/15 2016.
- [7] F. Wang *et al.*, "Latest advances in supercapacitors: from new electrode materials to novel device designs," *Chemical Society Reviews*, 10.1039/C7CS00205J vol. 46, no. 22, pp. 6816-6854, 2017.
- [8] A. O'Neill, U. Khan, and J. N. Coleman, "Preparation of High Concentration Dispersions of Exfoliated MoS₂ with Increased Flake Size," *Chemistry of Materials*, vol. 24, no. 12, pp. 2414-2421, 2012/06/26 2012.
- [9] X. Li, G. Wu, X. Liu, and W. Li, "Orderly Integration of Porous TiO₂(B) Nanosheets into Bunchy Hierarchical Structure for High-Rate and Ultralong-Lifespan Lithium-ion Batteries," *Nano Energy*, vol. 31, pp. 1-8, 01/01 2017.
- [10] T. Christen, "Ragone plots and discharge efficiency-power relations of electric and thermal energy storage devices," *Journal of Energy Storage*, vol. 27, p. 101084, 2020/02/01/ 2020.

- [11] A. Dehghani-sani, M. Dusseault, E. Tharumalingam, and R. Fraser, "Study of energy storage systems and environmental challenges of batteries," *Renewable and Sustainable Energy Reviews*, vol. 104, pp. 192-208, 04/01 2019.
- [12] B. Sun *et al.*, "Design strategies to enable the efficient use of sodium metal anodes in high-energy batteries," vol. 32, no. 18, p. 1903891, 2020.
- [13] N. Sazali, W. N. Wan Salleh, A. S. Jamaludin, and M. N. J. M. Mhd Razali, "New perspectives on fuel cell technology: A brief review," vol. 10, no. 5, p. 99, 2020.
- [14] T. Bhat, P. Patil, and R. J. J. o. E. S. Rakhi, "Recent trends in electrolytes for supercapacitors," vol. 50, p. 104222, 2022.
- [15] M. Waqas Hakim, S. Fatima, S. Rizwan, and A. Mahmood, "Pseudo-capacitors: Introduction, Controlling Factors and Future," in *Nanostructured Materials for Supercapacitors*: Springer, 2022, pp. 53-70.
- [16] S. Faraji, F. N. J. R. Ani, and S. E. Reviews, "The development supercapacitor from activated carbon by electroless plating—A review," vol. 42, pp. 823-834, 2015.
- [17] S. Xie, S. Liu, F. Cheng, and X. J. C. Lu, "Recent Advances toward Achieving High-Performance Carbon-Fiber Materials for Supercapacitors," vol. 5, no. 4, pp. 571-582, 2018.
- [18] Y. Yao, Y. Xu, B. Wang, W. Yin, H. J. P. Lu, and R. Technology, "Recent development in electrospun polymer fiber and their composites with shape memory property: a review," 2018.
- [19] A. Borenstein, O. Hanna, R. Attias, S. Luski, T. Brousse, and D. J. J. o. M. C. A. Aurbach, "Carbon-based composite materials for supercapacitor electrodes: a review," vol. 5, no. 25, pp. 12653-12672, 2017.
- [20] M. Poletto, H. L. Ornaghi Junior, and A. J. J. M. Zattera, "Native cellulose: structure, characterization and thermal properties," vol. 7, no. 9, pp. 6105-6119, 2014.
- [21] Y. Li *et al.*, "Purification and characterization of polysaccharides degradases produced by *Alteromonas* sp. A321," *International Journal of Biological Macromolecules*, vol. 86, pp. 96-104, 2016/05/01/ 2016.
- [22] T. Purkait, G. Singh, M. Singh, D. Kumar, and R. S. J. S. r. Dey, "Large area few-layer graphene with scalable preparation from waste biomass for high-performance supercapacitor," vol. 7, no. 1, p. 15239, 2017.

- [23] T. Purkait, G. Singh, M. Singh, D. Kumar, and R. S. Dey, "Large area few-layer graphene with scalable preparation from waste biomass for high-performance supercapacitor," *Scientific Reports*, vol. 7, no. 1, p. 15239, 2017/11/10 2017.
- [24] S. S. Shams, L. S. Zhang, R. Hu, R. Zhang, and J. J. M. L. Zhu, "Synthesis of graphene from biomass: a green chemistry approach," vol. 161, pp. 476-479, 2015.
- [25] H. Muramatsu *et al.*, "Rice husk-derived graphene with nano-sized domains and clean edges," vol. 10, no. 14, pp. 2766-2770, 2014.
- [26] D. Puthusseri, V. Aravindan, S. Madhavi, S. J. E. Ogale, and E. Science, "3D micro-porous conducting carbon beehive by single step polymer carbonization for high performance supercapacitors: the magic of in situ porogen formation," vol. 7, no. 2, pp. 728-735, 2014.
- [27] T. A. Khan *et al.*, "Hydrothermal carbonization of lignocellulosic biomass for carbon rich material preparation: A review," vol. 130, p. 105384, 2019.
- [28] Z. Li, W. Lv, C. Zhang, B. Li, F. Kang, and Q.-H. J. C. Yang, "A sheet-like porous carbon for high-rate supercapacitors produced by the carbonization of an eggplant," vol. 92, pp. 11-14, 2015.
- [29] S. Y. Lu, M. Jin, Y. Zhang, Y. B. Niu, J. C. Gao, and C. M. J. A. e. m. Li, "Chemically exfoliating biomass into a graphene-like porous active carbon with rational pore structure, good conductivity, and large surface area for high-performance supercapacitors," vol. 8, no. 11, p. 1702545, 2018.
- [30] M. Karuppanan, Y. Kim, Y.-E. Sung, and O. J. J. J. o. A. E. Kwon, "Nitrogen and sulfur co-doped graphene-like carbon sheets derived from coir pith bio-waste for symmetric supercapacitor applications," vol. 49, pp. 57-66, 2019.
- [31] A. Primo, P. Atienzar, E. Sanchez, J. M. Delgado, and H. J. C. c. García, "From biomass wastes to large-area, high-quality, N-doped graphene: catalyst-free carbonization of chitosan coatings on arbitrary substrates," vol. 48, no. 74, pp. 9254-9256, 2012.
- [32] H. Wang *et al.*, "Interconnected carbon nanosheets derived from hemp for ultrafast supercapacitors with high energy," vol. 7, no. 6, pp. 5131-5141, 2013.
- [33] M. Wahid, D. Puthusseri, D. Phase, S. J. E. Ogale, and fuels, "Enhanced capacitance retention in a supercapacitor made of carbon from sugarcane bagasse by hydrothermal pretreatment," vol. 28, no. 6, pp. 4233-4240, 2014.

- [34] L. Wang *et al.*, "Porous graphitic carbon nanosheets derived from cornstalk biomass for advanced supercapacitors," vol. 6, no. 5, pp. 880-889, 2013.
- [35] M. Liu, K. Zhang, M. Si, H. Wang, L. Chai, and Y. J. C. Shi, "Three-dimensional carbon nanosheets derived from micro-morphologically regulated biomass for ultrahigh-performance supercapacitors," vol. 153, pp. 707-716, 2019.
- [36] Z. Sun *et al.*, "From biomass wastes to vertically aligned graphene nanosheet arrays: A catalyst-free synthetic strategy towards high-quality graphene for electrochemical energy storage," vol. 336, pp. 550-561, 2018.
- [37] R. Mehdi, S. R. Naqvi, A. H. Khoja, and R. Hussain, "Biomass derived activated carbon by chemical surface modification as a source of clean energy for supercapacitor application," *Fuel*, vol. 348, p. 128529, 2023/09/15/ 2023.
- [38] M. Panahi-Kalamuei, O. Amiri, M. J. J. o. M. R. Salavati-Niasari, and Technology, "Green hydrothermal synthesis of high quality single and few layers graphene sheets by bread waste as precursor," vol. 9, no. 3, pp. 2679-2690, 2020.
- [39] J. Xu *et al.*, "Preparing two-dimensional microporous carbon from Pistachio nutshell with high areal capacitance as supercapacitor materials," vol. 4, no. 1, p. 5545, 2014.
- [40] P. C. Bhomick, A. Supong, R. Karmaker, M. Baruah, C. Pongener, and D. J. K. j. o. c. e. Sinha, "Activated carbon synthesized from biomass material using single-step KOH activation for adsorption of fluoride: Experimental and theoretical investigation," vol. 36, pp. 551-562, 2019.
- [41] S. Sankar *et al.*, "Biomass-derived ultrathin mesoporous graphitic carbon nanoflakes as stable electrode material for high-performance supercapacitors," vol. 169, p. 107688, 2019.
- [42] Y.-H. Chiu and L.-Y. J. J. o. t. t. i. o. c. e. Lin, "Effect of activating agents for producing activated carbon using a facile one-step synthesis with waste coffee grounds for symmetric supercapacitors," vol. 101, pp. 177-185, 2019.
- [43] F. Zhang *et al.*, "A high-performance supercapacitor-battery hybrid energy storage device based on graphene-enhanced electrode materials with ultrahigh energy density," *Energy & Environmental Science*, 10.1039/C3EE40509E vol. 6, no. 5, pp. 1623-1632, 2013.

- [44] Y. Guo and D. A. Rockstraw, "Activated carbons prepared from rice hull by one-step phosphoric acid activation," *Microporous and Mesoporous Materials*, vol. 100, no. 1, pp. 12-19, 2007/03/23/ 2007.
- [45] R. S. Dey, S. Hajra, R. K. Sahu, C. R. Raj, and M. K. Panigrahi, "A rapid room temperature chemical route for the synthesis of graphene: metal-mediated reduction of graphene oxide," *Chemical Communications*, 10.1039/C2CC16031E vol. 48, no. 12, pp. 1787-1789, 2012.
- [46] D. S. Yuan, J. Zeng, J. Chen, and Y. Liu, "Highly Ordered Mesoporous Carbon Synthesized via in Situ Template for Supercapacitors," *International Journal of Electrochemical Science*, vol. 4, no. 4, pp. 562-570, 2009/04/01/ 2009.
- [47] E.-P. Ng and S. Mintova, "Quantitative moisture measurements in lubricating oils by FTIR spectroscopy combined with solvent extraction approach," *Microchemical Journal*, vol. 98, no. 2, pp. 177-185, 2011/07/01/ 2011.
- [48] Y. Zhang and Z. Tang, "Porous carbon derived from herbal plant waste for supercapacitor electrodes with ultrahigh specific capacitance and excellent energy density," *Waste Management*, vol. 106, pp. 250-260, 2020/04/01/ 2020.
- [49] N. Guo, M. Li, Y. Wang, X. Sun, F. Wang, and R. Yang, "Soybean Root-Derived Hierarchical Porous Carbon as Electrode Material for High-Performance Supercapacitors in Ionic Liquids," (in eng), *ACS Appl Mater Interfaces*, vol. 8, no. 49, pp. 33626-33634, Dec 14 2016.
- [50] Z. Sun *et al.*, "From biomass wastes to vertically aligned graphene nanosheet arrays: A catalyst-free synthetic strategy towards high-quality graphene for electrochemical energy storage," *Chemical Engineering Journal*, vol. 336, pp. 550-561, 2018/03/15/ 2018.
- [51] S. Song, F. Ma, G. Wu, D. Ma, W. Geng, and J. Wan, "Facile self-templating large scale preparation of biomass-derived 3D hierarchical porous carbon for advanced supercapacitors," *Journal of Materials Chemistry A*, 10.1039/C5TA04721H vol. 3, no. 35, pp. 18154-18162, 2015.
- [52] J.-s. Lee *et al.*, "Metal–Air Batteries with High Energy Density: Li–Air versus Zn–Air," *Advanced Energy Materials*, vol. 1, pp. 34-50, 01/01 2011.
- [53] C. Liu, Z. Yu, D. Neff, A. Zhamu, and B. Z. Jang, "Graphene-based supercapacitor with an ultrahigh energy density," (in eng), *Nano Lett*, vol. 10, no. 12, pp. 4863-8, Dec 8 2010.

- [54] A. B. Fuertes and M. Sevilla, "Superior capacitive performance of hydrochar-based porous carbons in aqueous electrolytes," (in eng), *ChemSusChem*, vol. 8, no. 6, pp. 1049-57, Mar 2015.
- [55] J. L. Qi, X. Wang, J. H. Lin, F. Zhang, J. C. Feng, and W.-D. Fei, "A high-performance supercapacitor of vertically-oriented few-layered graphene with high-density defects," *Nanoscale*, 10.1039/C4NR07284G vol. 7, no. 8, pp. 3675-3682, 2015.
- [56] M. Biswal, A. Banerjee, M. Deo, and S. Ogale, "From dead leaves to high energy density supercapacitors," *Energy & Environmental Science*, 10.1039/C3EE22325F vol. 6, no. 4, pp. 1249-1259, 2013.
- [57] W. Qian *et al.*, "Human hair-derived carbon flakes for electrochemical supercapacitors," *Energy & Environmental Science*, 10.1039/C3EE43111H vol. 7, no. 1, pp. 379-386, 2014.
- [58] H. Feng *et al.*, "Hierarchical structured carbon derived from bagasse wastes: A simple and efficient synthesis route and its improved electrochemical properties for high-performance supercapacitors," *Journal of Power Sources*, vol. 302, pp. 164-173, 2016/01/20/ 2016.
- [59] J. Deng *et al.*, "Inspired by bread leavening: one-pot synthesis of hierarchically porous carbon for supercapacitors," *Green Chemistry*, 10.1039/C5GC00523J vol. 17, no. 7, pp. 4053-4060, 2015.
- [60] L. Zhou, H. Cao, S. Zhu, L. Hou, and C. J. G. C. Yuan, "Hierarchical micro-/mesoporous N-and O-enriched carbon derived from disposable cashmere: a competitive cost-effective material for high-performance electrochemical capacitors," vol. 17, no. 4, pp. 2373-2382, 2015.
- [61] C. Zhong, Y. Deng, W. Hu, J. Qiao, L. Zhang, and J. Zhang, "A review of electrolyte materials and compositions for electrochemical supercapacitors," *Chemical Society Reviews*, 10.1039/C5CS00303B vol. 44, no. 21, pp. 7484-7539, 2015.
- [62] X. Li and B. J. N. E. Wei, "Supercapacitors based on nanostructured carbon," vol. 2, no. 2, pp. 159-173, 2013.
- [63] Y. Myung, S. Jung, T. T. Tung, K. M. Tripathi, and T. Kim, "Graphene-Based Aerogels Derived from Biomass for Energy Storage and Environmental Remediation," *ACS Sustainable Chemistry & Engineering*, vol. 7, no. 4, pp. 3772-3782, 2019/02/18 2019.

- [64] L. Sun *et al.*, "From coconut shell to porous graphene-like nanosheets for high-power supercapacitors," *Journal of Materials Chemistry A*, 10.1039/C3TA10897J vol. 1, no. 21, pp. 6462-6470, 2013.
- [65] M. Wahid, D. Puthusseri, D. Phase, and S. Ogale, "Enhanced Capacitance Retention in a Supercapacitor Made of Carbon from Sugarcane Bagasse by Hydrothermal Pretreatment," *Energy & Fuels*, vol. 28, no. 6, pp. 4233-4240, 2014/06/19 2014.
- [66] C. Wang, D. Wu, H. Wang, Z. Gao, F. Xu, and K. Jiang, "A green and scalable route to yield porous carbon sheets from biomass for supercapacitors with high capacity," *Journal of Materials Chemistry A*, 10.1039/C7TA07579K vol. 6, no. 3, pp. 1244-1254, 2018.
- [67] Y. Wang *et al.*, "Three-dimensional honeycomb-like porous carbon derived from tamarisk roots via a green fabrication process for high-performance supercapacitors," *Ionics*, vol. 25, no. 9, pp. 4315-4323, 2019/09/01 2019.
- [68] M. Liu, K. Zhang, M. Si, H. Wang, L. Chai, and Y. Shi, "Three-dimensional carbon nanosheets derived from micro-morphologically regulated biomass for ultrahigh-performance supercapacitors," *Carbon*, vol. 153, pp. 707-716, 2019/11/01/ 2019.